Fall 12-8-2014

Examining the Role of DAX-1 in Regulation of Cell Proliferation in Human Breast Cells

Amy E. Scandurra
University of San Francisco, amyscandurra@gmail.com

Abstract

DAX-1 is a member of the Nuclear Hormone Receptor superfamily and acts as a transcriptional repressor. DAX-1 plays an important role in the development of adrenal and gonadal tissues. In addition to its role in normal cell development and differentiation, DAX-1 appears to have some influence on the progression of cancer. This work aims to examine the role of DAX-1 in regulation of proliferation in breast cancer. In our study, we have expressed DAX-1 in a DAX-1 deficient breast cancer cell line as well as knocked down DAX-1 expression in normal DAX-1 positive breast cells. Through these experiments, we were able to identify DAX-1 target genes and effect a change in proliferation rate.

In an effort to better understand DAX-1 function both in normal and disease states we also examined one type of posttranslational modification, SUMOylation. SUMOylation involves the addition of the small polypeptide conjugate SUMO (**S**mall **U**biquitin-like **Mo**difier) to proteins. SUMOylation can have a variety of effects on target proteins including changes in localization, protein-protein interaction, interaction with DNA, and in some cases stabilization of the target protein. SUMOylation of nuclear hormone receptors can have profound effects on their function. To study the effects of SUMOylation on DAX-1, the overall SUMOylation status of DAX-1 in mammalian cell lines was determined. It was found that DAX-1 is SUMOylated in several cell lines, both normal and carcinoma cells. Mutations were made in putative SUMOylation sites within the DAX-1 gene. Mutants were then transfected and assayed for changes in gene expression and activity. It was determined that mutating either of two putative SUMOylation sites led to a loss of DAX-1 repressive function when compared to wild-type DAX-1.

Table of Contents

Page Number

Acknowledgements

Principal Investigator

Dr. Christina Tzagarakis-Foster

Thesis Committee Members

Dr. James Sikes

Dr. Mary Jane Niles

Tzagarakis-Foster Laboratory

Hai Nguyen

Anthony Torres

Alexandra Maramba

Michael Heskett

Zachary Gallegos

Victor Gavallos

University of San Francisco Biology Graduate Students

Cendy Valle Oseguera, Carolyn Tu, Robin Bishop, Vivian Young

University of San Francisco Biology Department Faculty and Staff

Many thanks to lab manager Jeff Oda for all of his help.

Thanks to: USF Faculty Development Fund, Lily Drake Foundation

A very special thank you to my mentor and PI Christina Tzagarakis-Foster, Hai P. Nguyen who was a tremendous help in completing this work, as well as my grandfather Harry P. Aubright for his continued support and encouragement.

List of Figures

List of Tables

List of Abbreviations

A:	Alanine
ACTH:	Adrenocorticotropic hormone
AHC:	Adrenal Hypoplasia Congenita
AR:	Androgen Receptor
CCND1:	Cyclin D1
cDNA:	Complimentary DNA
Co-IP:	Co-Immunoprecipitation
DAX-1:	Dosage Sensitive Sex Reversal Adrenal Hypoplasia Congenita X Chromosome, Gene 1
DBD:	DNA Binding Domain
DHT:	5-α-dihydrotestosterone
DM:	Double Mutant
DMEM:	Dulbecco's Modified Eagle Medium
DNA:	Deoxyribonucleic Acid
DSS:	Dosage Sensitive Sex Reversal
E_2:	Estradiol
EDTA:	Ethylenediaminetetraacetic Acid
ER:	Estrogen Receptor
ERα:	Estrogen Receptor alpha
ERβ:	Estrogen Receptor beta
ERE:	Estrogen Response Element

FAS:	Fas Cell Surface Death Receptor
FBS:	Fetal Bovine Serum
FITC:	Fluorescein Isothiocyanate
GAPDH:	Glyceraldehyde 3-Phosphate Dehydrogenase
Her2:	Receptor Tyrosine-protein Kinase erbB-2
HH:	Hypogonadotropic Hypogonadism
HRE:	Hormone Response Element
HPAG:	Hypothalamic-Pituitary-Adrenal-Gonadal Axis
K:	Lysine
Ki-67:	Antigen KI-67
LBD:	Ligand Binding Domain
L0:	Lipid Only
LRH-1:	Liver Receptor Homolog-1
MCM7:	Minichromosome Maintenance Complex Component 7
mRNA:	Messanger RNA
NEAA:	Non-essential Amino Acids
N-CoR:	Nuclear Receptor Co-Repressor 1
NHR:	Nuclear Hormone Receptor
NR:	Nuclear Receptor
NT:	Non-targeting
Nur77:	Nerve Growth Factor IB
PBS:	Phosphate Buffered Saline
PCR:	Polymerase Chain Reaction

PI:	Propidium Iodide
PR:	Progesterone Receptor
PVDF:	Polyvinylidene Flouride
qPCR:	Quantitative Polymerase Chain Reaction
R:	Arginine
RanGAP1:	Ran GTPase-activating Protein 1
RNA:	Ribonucleic Acid
RNAi:	RNA Interference
SENP:	Sentrin-specific Proteases
SF-1:	Steroidogenic Factor-1
siRNA:	Short Interfering RNA
SMRT:	Silencing Mediator of Retinoid-Thyroid Receptor
SUSP1:	SUMO-specific Protease
SRY:	Sex Determining Region Y
StAR:	Steroidogenic Acute Regulator Protein
PIAS:	Protein Inhibitor of Activated STAT, SUMO-protein Ligase PIAS
SUMO:	Small Ubiquitin-like Modifier
TBS:	Tris Buffered Saline
UBA2:	Ubiquitin-like 1-Activating Enzyme E1B
UBC9:	SUMO-conjugating Enzyme
Ulp:	Ubiquitin-like Protease
UT:	Untreated
VC:	Vehicle Control

TOP2A: Topoisomerase II-alpha

WT: Wild-type

WT-1: Wilms' Tumor 1

Chapter 1: General Introduction

NHR overview

Nuclear hormone receptors (NHR) are ligand activated transcription factors that act as on-off switches to drive the expression or repression of target genes [1]. These proteins make up the largest family of eukaryotic transcription factors and regulate a diverse range of functions in the body including regulation of metabolic homeostasis, development and differentiation, reproductive development and maintenance of adult reproductive tissues, as well as salt balance [2]. Nuclear hormone receptors bind to specific sequences of DNA found upstream of target genes called hormone response elements (HRE). NHRs form dimers on the HREs and these dimers can be either homomeric, meaning they are comprised of two identical receptor monomers, or heteromeric and made up of two different types of receptor monomers. NHRs typically contain two conserved domains: a DNA binding domain (DBD) and a ligand binding domain (LBD). Ligands bound by NHRs include both steroid hormones, such as estrogen and testosterone, as well as nonsteroid hormones such as retinoic acid, thyroid hormone, and vitamin D [1]. To become activated, a ligand binds to the LBD of a nuclear hormone receptor resulting in a conformational change that allows the NHR/ligand complex to bind DNA at a HRE and regulate expression of a specific target gene. Typically, binding of a NHR can trigger the recruitment of other transcription factors, resulting in activation and expression of the target gene. However, NHRs can also act as negative regulators and alter the activity of other transcription factors leading to a reduction in expression of target genes.

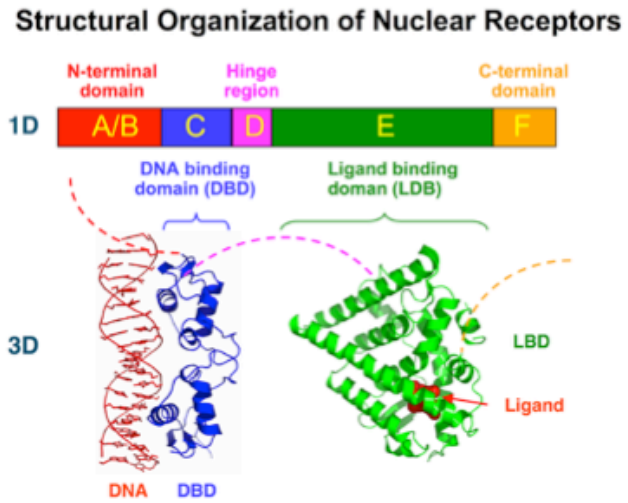

Figure 1-1 Typical nuclear hormone receptor structure.
Diagram showing the typical structure of an NHR. 1D shows amino acid sequence of conserved domains of a nuclear receptor: N-terminal domain (A/B), DNA binding domain (C), flexible hinge region (D), ligand binding domain (E), and the C-terminal domain (F). 3D shows crystallographic structures of DNA binding domain and ligand binding domain. (Boghog2. *Nuclear Receptor Structure*.12/03/2014. http://commons.wikimedia.org/wiki/File:Nuclear_Receptor_Structure.png)

Currently, there are 48 known nuclear hormone receptors in humans including receptors for which the ligands are known, adopted orphans for which the ligands were previously unknown, and orphan receptors for which there is no known ligand [3].

NHR Structure

The typical NHR consists of a variable N-terminal region, a conserved DNA binding domain (DBD), a hinge or linker region, a conserved ligand-binding domain (LBD), and a highly variable C-terminal domain, as shown in Figure 1-1 [4]. The N-terminal region varies among NHRs and contains a region that has ligand-independent transcriptional activity termed the activation function 1 (AF-1) [5]. The DBD gives NHRs their specificity in binding to hormone response elements (HRE) within the DNA. The DBD of an NHR typically binds two hexameric nucleotide sequences, called half-sites, that compose the HRE [6]. NHRs can bind as monomers to a single half-site, or as homodimers or heterodimers to a set of two half-sites. Specificity of binding between NHRs and the DNA of a HRE is conferred by the nucleotide sequence present in a given half-site, the relative orientation of half-site pairs, and the amount of space between half-sites [6, 7]. These three factors determine whether a monomer, homodimer, or heterodimer pair of nuclear hormone receptors will bind. The DBD is composed of two zinc finger motifs, each made up of approximately 70 amino acids forming two α-helices oriented perpendicularly from one another as seen in Figure 1-2. Zinc fingers mediate protein binding to HREs and help to stabilize the NHR complex [8]. Connecting the DBD to the LBD is a hinge region that allows flexibility of the protein so that it can interact with both ligands bound to the LBD and to response elements in the DNA at the same time.

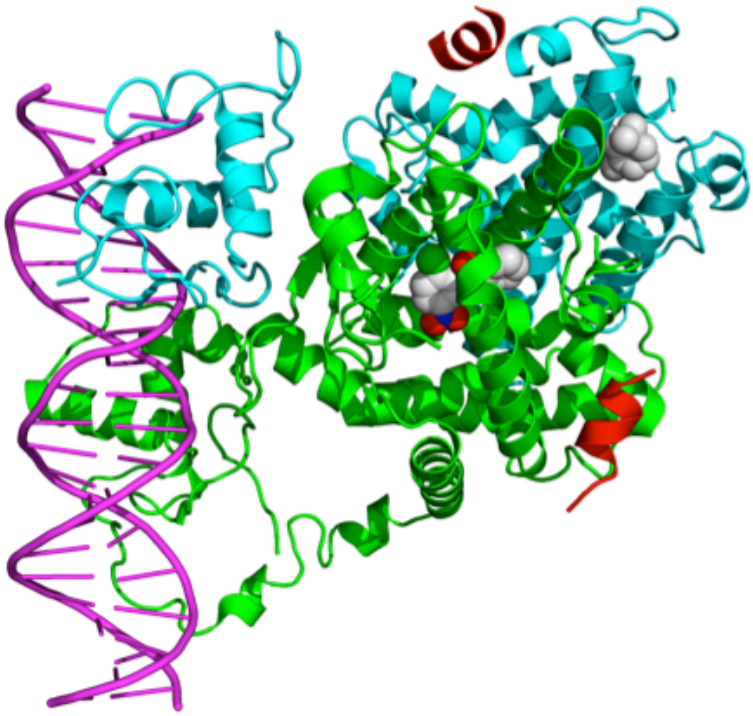

Figure 1-2 DNA binding domain bound to HRE in DNA.
The zinc fingers of a heteromeric pair of a nuclear hormone receptors binding to the DNA half site within a hormone response element (HRE) in double stranded DNA.
(Boghog2. *PPARg RXRa*.12/03/2014.
http://commons.wikimedia.org/wiki/File:PPARg_RXRa_3E00.png)

Structurally the ligand-binding domain is composed of three layers of α-helices that run antiparallel to one another forming what is known as the α-helical sandwich fold. The α-helical sandwich is made up of three antiparallel α-helices forming the "filling" surrounded by two additional α-helices on one side and three on the other forming the "bread". The innermost layer of α-helices forms a cavity that acts as the ligand-binding pocket as shown in Figure 1-3 [3]. Although the LBD is considered the most highly conserved domain in the nuclear hormone receptor family, the ligand-binding pocket is one of the least conserved regions among NHRs as this region is responsible for the specificity of ligand binding [3]. Ligands vary greatly among the NHRs, so there is considerable variation in the sequence specificity as well as size and shape of the ligand-binding pocket. A second activation domain (AF-2) is found within the LBD. Unlike the AF-1 domain, AF-2 domain is highly ligand dependent and is much less variable.

DAX-1: A Unique NHR

DAX-1 (Dosage sensitive sex-reversal adrenal hypoplasia X chromosome gene 1) encoded by the gene *NR0B1* is a unique member of the nuclear hormone receptor family. The NR0B1 gene has a relatively simple structure of two exons separated by a single intron that encodes a 470 amino acid protein as seen in Figure 1-4 [9]. Exon 1 contains 1168 base pairs, exon 2 contains 245 base pairs and the intron is 3385 base pairs [10]. The DAX-1 structure differs from that of the typical NHR, in that DAX-1 is an orphan receptor, and, as such, has no known ligand [1].

Figure 1-3 General ligand-binding domain crystallographic structure.
The ligand-binding domain consists of three layers of α-helices running antiparallel to one another, shown as colored ribbons. The innermost region of helices forms the ligand-binding pocket, shown filled with gray space filling ligand.
(Boghog2. *ROR3C.* 12/03/2014.http://commons.wikimedia.org/wiki/File:RORC_3L0L.png)

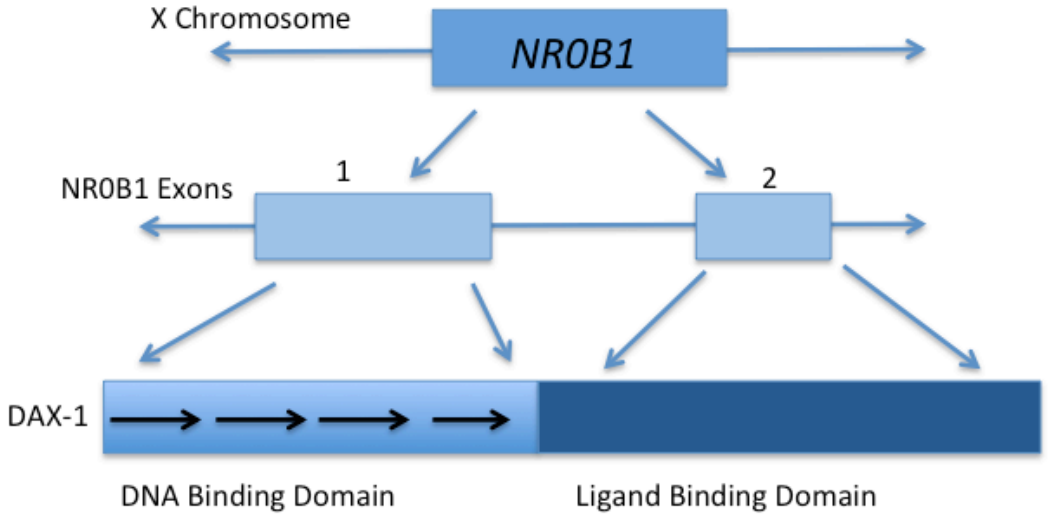

Figure 1-4 *NR0B1* and DAX-1 structure.
NR0B1 gene is located on the p arm of the X chromosome between positions 21.3 and 21.2. The gene consists of two exons that encode for a 470 amino acid protein: DAX-1. The DAX-1 protein consists of two regions, the DNA binding domain and the ligand binding domain.

In addition, DAX-1 lacks several of the typically conserved domains of NHRs. Rather than the conserved DBD containing two zinc fingers, the transactivational AF-1 site, and the typical hinge domain, DAX-1 contains alanine-glycine rich repeat sequences of 65-67 amino acids as well as three leucine motifs known as LXXLL boxes in the N terminal DBD region, as seen in Figure 1-5 [11, 12]. Additionally, the N-terminal domain of DAX-1 contains cysteine residues that are arranged in such a way that interaction with the zinc ion in zinc fingers of other nuclear hormone receptors is possible [13]. Though DAX-1 contains the conserved LBD, no ligand has been found to date. Examination into the structure of the ligand-binding pocket of DAX-1 has revealed that the typical hydrophobic core found in NHRs is absent. The result is the formation of a cavity that is much smaller than that of other NHRs, suggesting that no ligand is likely to be found for DAX-1 [1]. Therefore, DAX-1's function seems to be purely ligand independent.

DAX-1 Function

The DAX-1 protein acts as a coregulator and transcriptional repressor of other NHRs. Typically coactivators bind the AF-2 domain of an activated NHR. However, DAX-1 is able to bind this same domain and repress transcriptional activity [14]. Upon binding of the AF-2 domain, DAX-1 recruits corepressors such as N-CoR and Alien to the promoter region of target genes [15]. This type of repression mechanism is observed with multiple NHRs, such as estrogen receptor (ER) and liver receptor homolog 1 (LRH-1) as seen in Figure 1-6 [16]. Interaction with NHRs is thought to be mediated through the third LXXLL box as this box in particular has sequence homology to the AF-2 domain of other nuclear hormone receptors [17]. Mutation of this box results in an inability of DAX-1 to recruit

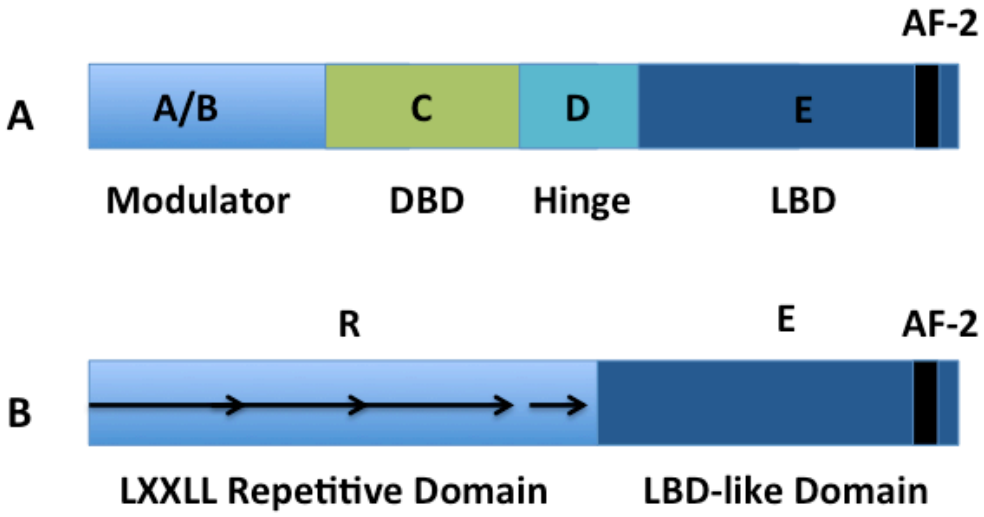

Figure 1-5 Comparison of typical NHR structure with DAX-1 structure.
A: Typical NHR structure with regions A-E (previously described Figure 1-1)
B: DAX-1 structure with repetitive domain (R) containing LXXLL repeat motif boxes and ligand binding-like domain (E).

and bind corepressors as well as the loss of repressive ability of DAX-1 on protein targets like steroidogenic factor 1 (SF-1) and ER [17]. This type of repressive interaction has been shown between DAX-1 and SF-1 [12, 18, 19]. SF-1, along with Wilms' tumor 1 (WT1), is involved in the development of the gonads and regulates a number of target genes responsible for development of the testes [20]. DAX-1 and the corepressor Nuclear Receptor-corepressor (N-CoR) act together to repress SF-1/WT1 transcriptional activity [18]. Additionally, it has been proposed that DAX-1 inhibits another testes specific factor, Nur77 [21]. For these reasons DAX-1 is considered to be an anti-testes factor. Additionally, DAX-1 has been shown to inhibit the transcriptional activity of a broad range of other nuclear hormone receptors including estrogen receptor (ER)[17], progesterone receptor (PR)[22], liver receptor homologue-1 (LRH-1)[17], and androgen receptor (AR)[22].

Another mode of repressional activity by DAX-1 can occur when NHR are inactive and have no ligand bound. DAX-1 contains a C-terminal transcriptional silencing domain that allows it to interact with corepressors such as N-CoR, silencing mediator of retinoid-thyroid receptor (SMRT), and Alien [21, 23]. This complex binds NHRs in the absence of ligand. In this state NHRs remain inactive and are unable to bind a ligand until a conformation change takes place.

The Role of DAX-1 in Physiological and Developmental Processes

DAX-1 plays a key role in the development and function of the adrenal gland and the hypothalamic-pituitary-gonadal axis. Mutations in the *NR0B1* gene can have serious impacts on the development of the adrenal glands and the gonadal tissues.

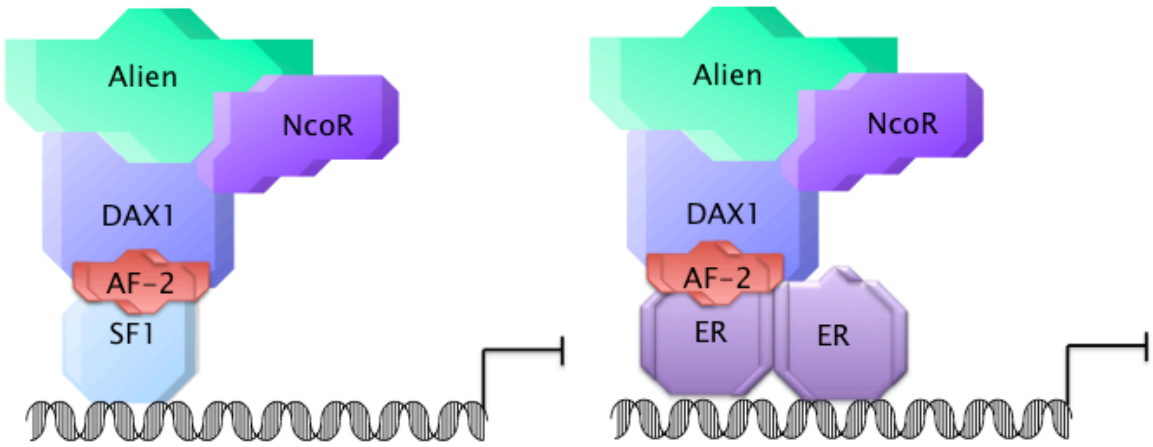

Figure 1-6 Mechanism of DAX-1 mediated repression.
The LXXLL box of DAX-1 binds the AF-2 domain of nuclear hormone receptors ER, SF-1, or others. DAX-1 recruits corepressors such as NCo-R and Alien. Corepressors bind to the promoter region of target genes and help to prevent transcription.
(Image: Hai P. Nguyen)

Adrenal hypoplasia congenita (AHC) is rare congenital disorder that is characterized by an underdeveloped adrenal cortex and severe adrenal insufficiency [24]. There are two histological forms of adrenal hypoplasia congenita, which has an estimated frequency of 1:12,500 live births [25]. The miniature adult form presents with smaller than normal adrenal glands and is associated with central nervous system deficiencies as well as abnormal pituitary development and function. This form, however, is not associated with DAX-1. The cytomegalic form of AHC is associated with mutations in the *NR0B1* gene. The adrenal gland develops with little or no cortex permanent zone and disorganized residual cortical tissue that contains vacuolated cells similar to those seen in the fetal adrenal cortex [25]. The result of these morphological differences is a nonfunctional adrenal cortex. The adrenal cortex is responsible for production of adrenal cortical steroid hormones, such as glucocorticoid, mineralocorticoid, and sex hormones. Without these hormones serious symptoms arise.

This form of AHC predominantly affects males due to the fact that it is an X-linked gene. Patients generally begin to exhibit symptoms in early childhood. These symptoms include extremely low salt levels, hypoglycemia, dehydration, decreased appetite, hypotension, decreased levels of glucocorticoids and aldosterone, and increased levels of adrenocorticotropic hormone (ACTH) [26]. Without required treatment of mineralocorticoid and glucocorticoid replacement therapy, AHC would be fatal. Hypogonadotropic hypogonadism (HH) is a condition that is associated with AHC that some patients also develop. HH involves a decrease in gonadatropic hormones thereby preventing normal sexual development during puberty [27]. Testosterone replacement is given to AHC patients also exhibiting hypogonadotropic hypogonadism. In addition to AHC and HH, DAX-1 has also been shown to play a role in normal sex determination and development of the gonads. Male to female sex reversal in

individuals with a normal sex determining region Y (SRY) gene has been mapped to a region of the X chromosome that includes *NR0B1*. For this reason the *NR0B1* gene is considered a likely candidate for causing dosage sensitive sex reversal (DSS) [25].

Normally DAX-1 functions in the hypothalamic-pituitary-adrenal-gonadal (HPAG) axis and is expressed in both developing as well as adult tissues. During development, DAX-1 is expressed in the adrenal cortex, anterior pituitary, hypothalamus, and the gonad. Whereas in adult tissues, DAX-1 expression has been seen in the adrenal cortex, Stertoli and Leydig cells of the testis, theca, granulosa, and interstitial cells of the ovary, as well as very specific locations in the anterior pituitary and hypothalamus [25, 28].

The expression of DAX-1 during both development and adulthood resembles that of another orphan nuclear hormone receptor, steroidogenic factor 1 (SF-1). SF-1 is well known for its regulatory role of the HPAG axis and is a transcriptional activator of genes in the steroid hormone biosynthesis pathway of the HPAG axis [28]. Similarly to what is seen with DAX-1, mutations in SF-1 can lead to adrenal failure and XY sex reversal. DAX-1 has been shown to repress SF-1 activity, thereby acting as an antagonist [28].

DAX-1 is a global negative repressor of genes in the steroid hormone production pathway. Steroidogenesis is an essential process for fundamental physiological functions such as metabolism, salt and water balance, and reproduction. Steroid hormone production occurs in a variety of tissues most notably the adrenal glands, ovaries, testes, and the brain [29]. All steroid hormones are synthesized from cholesterol and are derived through a series of enzymatic reactions [29]. The first step in this process takes place in the mitochondria and involves the delivery of cholesterol from the outer mitochondrial membrane to the inner mitochondrial membrane [30]. This is the rate-limiting step in the enzymatic process and requires mediation by

the steroidogenic acute regulatory (StAR) protein [31]. StAR production is triggered by steroidogenic stimuli such as adrenocorticotropic hormone (ACTH) and angiotensin II (AII) [32]. DAX-1 is one of the key modulators of StAR transcription and therefore plays an important role in the regulation of steroid hormone production. DAX-1 exerts this inhibition by binding the StAR promoter region leading to a drastic decrease in StAR transcription [33].

The Role of DAX-1 in Breast Cancer

The action of steroid hormones, most notably estrogens and progesterone, are extremely influential forces for the development and progression of breast cancer. Additionally, androgens can play a role in breast cancer because of their ability to be converted into estrogens [34]. Estrogen signaling in the breast plays a driving role in proliferation. There are two forms of ER, estrogen receptor alpha (ERα) and estrogen receptor beta (ERβ) [35]. Each is encoded by a different gene, but share similar homology. Additionally, the two forms of ER have somewhat different functions, with ERα being the primary form responsible for proliferation and growth [36]. Typically, estrogen receptor (ER) binds its ligand, estrogen (17β-estradiol), becomes active, translocates from the cytosol to the nucleus, and moves to estrogen response elements (ERE) in DNA. Estrogen receptor can form a homodimer with two receptors of one form, either ERα (αα) or ERβ (ββ) or form a heterodimer with one type of each receptor ERαβ [36]. The activated receptor can then drive transcription of target genes.

One important target gene of ER is Cyclin D1 (CCND1). Cyclin D1 is a critical cell cycle control protein whose transcriptional regulation is responsible for mediating the transition from G1 to S phase of the cell cycle [34]. Not only has over-expression of Cyclin D1 been shown to increase breast cancer growth, it also plays a driving role in breast cancer progression [37, 38].

Additionally, Cyclin D1 expression has also been linked to the development of resistance to tamoxifen antiestrogen therapy [39]. Cyclin D1 is a key proliferation target of estrogen receptor and drives progression through the cell cycle. ER positive breast cells proliferate in the presence of estrogen. Estrogen-dependent proliferation occurs in both normal, healthy cells and in cancer cells.

DAX-1 is a known repressor of estrogen receptor and has been show to reduce ER transcriptional activity [17]. Recent research has elucidated a relationship between estrogen receptor, androgen receptor, and DAX-1, showing that AR may repress ER activity by activating DAX-1 in estrogen-dependent breast cancer cells [40]. ERα positive cells treated with non-aromatizable androgen 5-α-dihydrotestosterone (DHT) had decreased Cyclin D1 expression and this reduction in Cyclin D was mediated through AR recruitment of DAX-1 [38, 40]. Increased transcription of DAX-1 by AR leads to inhibition of ER transcription of Cyclin D1, therefore slowing the rate of proliferation in breast cancer cells. Androgens have been shown to have a variety of effects on both normal and diseased states of the breast. Androgen signaling has primarily inhibitory effects on the growth of normal breast cells and appears to act as a protective force in breast cancer [41, 42]. Activation of AR by it's natural ligand dihydrotestosterone (DHT) or a synthetic analog significantly increased DAX-1 levels, resulting in an inhibition of the proliferation of MCF7 breast cancer cells [40]. However, in some studies androgens have been shown to enhance breast cancer development and growth [43].

Chapter 2: Examining the Role of DAX-1 in Regulating Proliferation in Breast Cancer

Chapter 2: Introduction

Previous research has shown that DAX-1 is a negative repressor of estrogen receptor transcriptional activity [40, 44]. However, the precise mechanism of repression and the complement of downstream target genes affected by DAX-1 activity are unknown. In estrogen receptor positive breast cancer, the binding of estrogen to ER drives proliferation through the cell cycle causing cells to divide and multiply. One of the mechanisms by which ER drives proliferation is by transcription of the Cyclin D1 gene. Cyclin D1 is a cell cycle control protein, which mediates the transition from G0/G1 into S phase of the cell cycle. During G0/G1 a cell is metabolically active, but is in arrest and it is not actively progressing through the cell cycle. However, in G1 a cell will begin the preparations for S phase. During DNA synthesis, or S phase, the DNA content of the cell is copied so that the cell can later divide into two new daughter cells. Accumulation of Cyclin D propels the cell through G1 and into S phase. Without enough Cyclin D present, the cell will not enter S phase of the cell cycle, but will stay arrested in G1. Previous research (Tzagarakis-Foster, unpublished) has shown that in a subset of breast cancer patients, DAX-1 is expressed in normal tissue of the breast, but expression is down regulated or absent in patient matched tumor tissue (Figure 2-1). This observation has led to the hypothesis that DAX-1 acts a protective force in breast cells and the loss of its expression can lead to a more proliferative phenotype.

To better understand the role of DAX-1 mediated repression and the downstream genes affected by its presence, I have examined both a DAX-1 deficient ER positive breast cancer cell line (MCF7) and a DAX-1 positive, ER negative normal epithelial breast cell line (MCF10A).

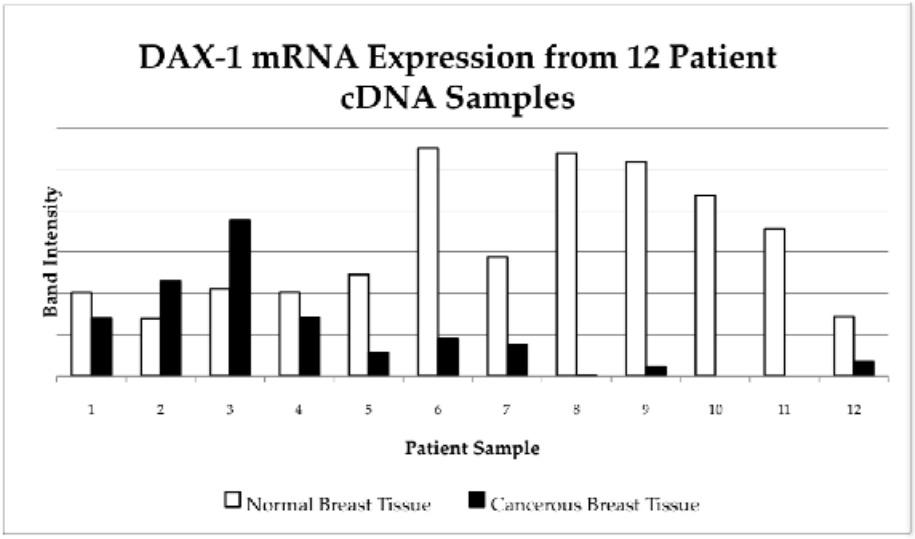

Figure 2-1 DAX-1 mRNA expression from 12 patient cDNA samples.
DAX-1 expression data from 12 patient samples. Normal breast tissues are shown with white bar, cancerous breast tissues are shown with dark bar. 10/12 patients had higher DAX-1 expression in normal tissue compared to cancer tissue. Expression level is measured by PCR band intensity from cDNA of patient samples.
(Data: Sean Judge)

In my research, I have ectopically expressed DAX-1 in MCF7 cells to determine the effect of DAX-1 on target gene expression and proliferation rate in the context of breast cancer. Additionally, I employed RNA interference technologies using small interfering RNAs (siRNAs) to selectively knockdown the expression of DAX-1 in MCF10A normal breast cells. I have compared the expression level of target genes when DAX-1 was highly expressed in breast cancer cells and when DAX-1 levels were reduced in normal breast cells. By elucidating the targets affected by DAX-1 in breast cancer cells, as well as normal breast cells, we hope to gain a better understanding of the larger role this unique nuclear hormone receptor may play in cancer.

Chapter 2: Materials and Methods

Cell Culture

All cell lines were routinely passaged, cultured, and maintained at 37° C in a humidified 5% CO_2 tissue culture incubator. MCF7 human breast cancer cells were cultured in Dulbecco's modified eagle medium (DMEM) or Ham's F12 (1:1) without phenol red. Phenol red is an estrogen and since MCF7 cells are estrogen receptor positive cells they are sensitive to phenol red. Media was supplemented with 10% Fetal Bovine Serum (ATCC, Manassas, VA), 1% L-Glutamine (Invitrogen, Carlsbad, CA), 1% Penicillin/Steptomycin (Invitrogen, Carlsbad, CA), 1% Fungizone (Invitrogen, Carlsbad, CA), and Bovine Insulin (Sigma-Aldrich, St. Louis, MO). MCF10A human mammary epithelial cells were cultured in Dulbecco's modified eagle medium (DMEM) or Ham's F12 (1:1) without phenol red. Media was supplemented with 5% Horse Serum (ATCC, Manassas, VA), 1% L-Glutamine (Invitrogen, Carlsbad, CA), 1% Penicillin/Steptomycin (Invitrogen, Carlsbad, CA), 1% Fungizone (Invitrogen, Carlsbad, CA), and 100ng/ml cholera toxin (Sigma-Aldrich, Saint Louis, MO). MDA-MB-231 human triple negative breast cancer cells were cultured in Dulbecco's modified eagle medium (DMEM) or Ham's F12 (1:1) with phenol red and supplemented with 10% Fetal Bovine Serum (ATCC, Manassas, VA), 1% L-Glutamine (Invitrogen, Carlsbad, CA), 1% NEAA (Invitrogen, Carlsbad, CA), (1% Penicillin/Steptomycin (Invitrogen, Carlsbad, CA), and 1% Fungizone (Invitrogen, Carlsbad, CA).

To passage and maintain cells, cells were first washed with phosphate buffered saline (PBS), treated with Trypsin-Versene (EDTA) and incubated at 37° C until released from flask. Cells were resuspended and passaged at a 1:8 ratio.

DNA Isolation

Plasmid DNA was isolated using PureYield Plasmid Miniprep System (Promega, Madison, WI) according to the manufacturer's instructions using a starting volume of 2 mL of bacterial culture. Purified DNA was measured using the NanoDrop 1000 Spectrophotometer (Thermo Scientific, Wilmington, DE) and sequenced (McLab, South San Francisco, CA) to confirm DNA sequences.

Viral Transfection

Adenoviral vectors (BD Biosciences Clonetech, San Jose, CA) containing either the DAX-1 gene or the LacZ gene (control) were transfected into MCF7 and MDA-MB-231 cells. Cells were plated in six well plates in serum free media and transfected with 1µl of adenovirus containing either DAX-1 or LacZ per 1mL of media. Cells were incubated with virus in serum free media for 24 hours to synchronize cells to the same phase of the cell cycle. Cells were then treated with estrogen to a final concentration of 10^{-7} M for 1-72 hours. Cells were collected for total RNA isolation and cDNA was synthesized.

Plasmid Transfection

pcDNA 3.1 plasmid (Life Technologies, Carlsbad, CA) containing either the an empty vector control or the wild-type DAX-1 DNA sequence was transfected into MCF7 cells seeded in six cell plates using a range of concentrations (1500-2000ng) of plasmid with 50µL of Lafectine RU50 transfection reagent (MednaBio, Burlingame, CA). Cells were incubated for 48 hours and collected for total RNA isolation and whole cell protein lysate.

siRNA Transfection

A set of three synthetic double stranded Stealth siRNA oligonucleotides targeting the DAX-1 gene were obtained from Life Technologies (Carlsbad, CA) (Table 2-1). The medium GC non-targeting Stealth oligonucleotide was used as a control. Six well plates were seeded at 500,000 cells per cell and reverse transfected using Lafectine RU50 (MednaBio, Burlingame, CA) and 300pmol concentration of control or targeting siRNAs. Cells were incubated for 48 hours and collected for total RNA isolation and whole cell protein lysate.

siRNA	**Sequence**	**Target Region**
DAX-1 siRNA 1	CCCAUGACAGAUUCAUCGAACUUAA UUAAGUUCGAUGAAUCUGUCAUGGG	Exon 2 Position 1290
DAX-1 siRNA 2	UCGGCACAGUCAGCAUGGAUGAUAU AUAUCAUCCAUGCUGACUGUGCCGA	Exon 2 Position 1383
DAX-1 siRNA 3	CAGUGGCAGGGCAGCAUCCUCUACA UGUAGAGGAUGCUGCCCUGCCACUG	Exon 1 Position 44

Table 2-1 siRNA sequences.

RNA Isolation and cDNA Synthesis

Total RNA was isolated using the RNeasy Mini Kit (Qiagen, Valencia, CA) as per the manufacturer's instruction, with the optional RNase-Free DNAse (Qiagen) step added to remove genomic DNA contamination. RNA was measured for concentration and purity using the NanoDrop 1000 Spectrophotometer (Thermo Scientific, Wilmington, DE). High Capacity cDNA Reverse Transcription Kit (Applied Biosystems, Foster City, CA) was used to synthesize cDNA

from the isolated RNA according to manufacturer's instructions. Thermocycling was carried out using MJ Mini Personal ThermoCycler (BioRad, Hercules, CA) with the following conditions.

	Step 1	**Step 2**	**Step 3**	**Step 4**
Temperature	25°C	37°C	85°C	4°C
Time	10 min	120 min	5 min	∞

Table 2-2 cDNA synthesis thermocycler conditions.

cDNA was then measured via NanoDrop diluted and normalized for subsequent PCR analysis.

Protein Isolation

Whole cell protein lysate was collected following 24 or 48-hour treatments using either NP-40 or RIPA lysis buffer (Boston BioProducts, Worcester, MA) with Halt Protease Inhibitor (Thermo Fisher Scientific, Rockford, IL) added at a concentration of 1:100. Cells were trypsinized and collected from 6 well plates and centrifuged at 14,000 g for 5 minutes. Supernatant was removed and pelleted cells were resuspended in lysis buffer and incubated on ice for 15 minutes. Samples were sonicated using Misonix Ultrasonic Liquid Processor (Misonix, Inc, Farmingdale, NY) at an amplitude of 50 for two pulses of 30 seconds with a 40 second pause between pulses. The lysate was centrifuged at 14,000 g for 10 minutes to pellet insoluble materials and the supernatant was transferred to a new tube and stored at -70°C for future analysis.

Western Blot

Western blots were performed using the XCell II Blot Module (Invitrogen, Carlsbad, CA) according to the NuPAGE Novex Bis-Tris Protocol (Invitrogen, Carlsbad, CA) using 4X

NuPAGE LDS sample loading buffer and 10X NuPAGE sample reducing agent. Samples were normalized using the Coomassie Plus Bradford Protein Assay (Thermo Fisher Scientific, Rockford, IL) and then combined with sample loading buffer and reducing-agent to a final volume of 30µL. Samples were run on gradient 4-12% Bis-Tris SDS-PAGE gels for 45 minutes at 200V on the XCell II Blot Module. Protein was transferred from gel to PVDF membrane according to manufacturer's protocol using XCell II Blot Module with blot apparatus. Transfer blots were run at 25V for 1 hour. Membranes were then blocked in 5% Blotto made in Tris-Buffered Saline with Tween 20 (TBST) for 1 hour with rocking at 150 RPM and incubated overnight at 4° C with primary antibody (listed below) made in 5% Blotto at 1:1000 dilution with rocking at 150 RPM. Membranes were washed with TBST for 10 minutes three times before secondary antibody application. Appropriate secondary antibody, either rabbit or mouse (BD Biosciences, San Jose, CA) was prepared in 5% Blotto made with TBST at 1:2000 dilution. Membranes were incubated in secondary antibody for one hour at room temperature with rocking at 150 RPM, and then washed with TBST for 10 minutes three times prior to developing. Western blots were developed using the chemiluminescence Thermo Scientific Kit and analyzed using the BioRad GelDoc System (BioRad, Hercules, CA).

Protein	**Species**	**Company**
DAX-1 (K-17)	Rabbit polyclonal	Santa Cruz Biotech Santa Cruz, CA
GAPDH	Mouse monoclonal	Santa Cruz Biotech Santa Cruz, CA
Cyclin D1 (N2C3)	Rabbit polyclonal	GeneTex Irvine, CA

Table 2-3 Antibodies.

Standard PCR and qPCR

cDNA made from extracted mRNA was used as template for standard PCR and qPCR. Samples for standard PCR were prepared using 12.5µL of 2X GoGreen (Promega, Madison, WI) or Taq 2X Master Mix (New England BioLabs, Ipswich, MA), 0.25µL of 10µM forward and reverse primers (listed in table 2-5), 12µL of dH2O, and 2µL cDNA. PCR was performed using MJ Mini Personal ThermoCycler (BioRad, Hercules, CA) using the protocol below with varying annealing temperatures.

Step	**Temp**	**Time**
Initial Denaturation	95°	4 minutes
30 Cycles: Denaturation Annealing Elongation	 95° 45-65° 72°	 30 sec 30 sec 30 sec
Final Extension	72°	4 minutes
Hold	4°	∞

Table 2-4 PCR thermocycler conditions.

Following PCR, samples were electrophoresed through a 1.5-2% 1X TAE agarose gel containing ethidium bromide. PCR products were visualized by ultraviolet light exposure using the BioRad GelDoc System (BioRad, Hercules, CA).

qPCR reactions were performed in triplicate using BioRad CFX96 Real-Time PCR system. qPCR reactions were prepared using 10.5 µL of SYBR Green Master Mix (Life Technologies, Carlsbad, CA), 0.25µL of 10µM forward and reverse primers (listed in table 2-5), 12µL of dH2O,

and 2μL cDNA. GAPDH housekeeping gene was used as control and experimental genes were compared to GAPDH as a baseline. Fold-change values were calculated by comparing untreated and transfected samples. Error bars on qPCR results represent standard deviation of the mean. Statistical significance was calculated by using one and two tailed T-tests comparing untreated and transfected groups. Data found to be statistically significant ($p < 0.05$) is indicated by asterisks.

Gene Name	**Fwd Primer 5'-3'**	**Rev Primer 5'-3'**	**Annealing Temp**
GAPDH	ACA GCC GCA TCT TCT TGT GCA	GGG CTT GAC TGT GCC GTT GAA	58° C
DAX-1	GAC TCC AGT GGG GAA CTC AG	ATG ATG GGC CTG AAG AAC AG	57° C
CyclinD1	TAG CAC CTT GGA TGG GTA ATT	ATC GTG CGG CAT TGC GGC	59° C
ERα	CCA CCA ACC AGTT GCA CCA TT	GCG AGT CTC CTT GGC AGA TCC	54° C
Ki-67	ACA GAC CTC AAG AGC TTG CC	CCA GGG ATG CCT TCA ACT GT	57° C
MCM7	TGG CAC TGA AGG ACT ACG	CTG AGG CAG CAG CTC TTG TA	56° C
TOP2A	TGG GGT CCT GCC TGT TTA GT	TGT CTG GGC GGA GCA AAA TA	55° C

Table 2-5 PCR Primers.

Cell Cycle Analysis

MCF7 and MCF10A cells were grown in 6 well plates and transfected with either plasmids or siRNAs (previously described). Cells were collected and pelleted by centrifugation at 5,000 g for 5 minutes, resuspended and washed in 500µL 1X PBS, and centrifuged at 5,000 g for 5 minutes. Supernatant was removed, cells were resuspended in 50µL PBS, and mixed with 500µL of 100% ethanol. Cells were stored overnight at -20°C. Cells were centrifuged at 5,000 g for 5 minutes and supernatant was removed. Cells were resuspended with 100 µL PI/RNase Staining Buffer (BD Pharmingen, San Diego, CA), 10µL Propidium Iodide Staining Solution (BD Biosciences, San Jose, CA) was added and incubated for 10 minutes before analysis by flow cytometry. The BD Acurri C6 (BD Biosciences, San Jose, CA) flow cytometer was used to analyze samples. Cell cycle analysis samples were run in duplicate. Statistical significance calculated by using two tailed T-test comparing untreated and transfected groups. Data found to be statistically significant ($p < 0.05$) is indicated by asterisks.

Chapter 2: Results

Expression of DAX-1 in human breast adenocarcinoma cells (MCF7) by viral transfection.

A schematic of the workflow used for the following experiment is shown in Figure 2-2. MCF7 cells were serum-starved for 24 hours before being infected with control adenovirus containing the lacZ gene or adenovirus containing the DAX-1 gene (BD Biosciences Clonetech, San Jose, CA). After 24 hours exposure to virus, the cells were treated with estradiol (E_2) to a final concentration of 10^{-7} M for a designated number of hours. After treatment with E_2 cells were collected and total RNA was isolated and cDNA was synthesized. Finally, cDNA was analyzed using standard PCR.

Considering the known repressional activity of DAX-1 on estrogen receptor and the role of ER in transcription of the cell cycle control protein, Cyclin D1, I wished to initially examine the effect of DAX-1 expression of Cyclin D1. It was found that the introduction of DAX-1 expression into the MCF7 breast cancer cells resulted in a decrease in the amount of detectable ERα as well as Cyclin D1 (Figure 2-3). Since a decrease was seen in Cyclin D1, a key regulator of the progression from G1 into S phase of the cell cycle (Figure 2-4), I next wanted to determine if a change in proliferation level could be detected. Cell proliferation level was examined using a luciferase viability assay. Cells were transfected as described previously and treated with E_2 for up to 72 hours. It was determined that the addition of DAX-1 not only decreased proliferation of MCF7 cells, but that cells regressed beyond the starting point (Figure 2-5 a). These data supports what was seen previously with the PCR expression data. A decrease in ERα and Cyclin D1 expression should lead to a decrease in proliferation, since an ample concentration of Cyclin D1

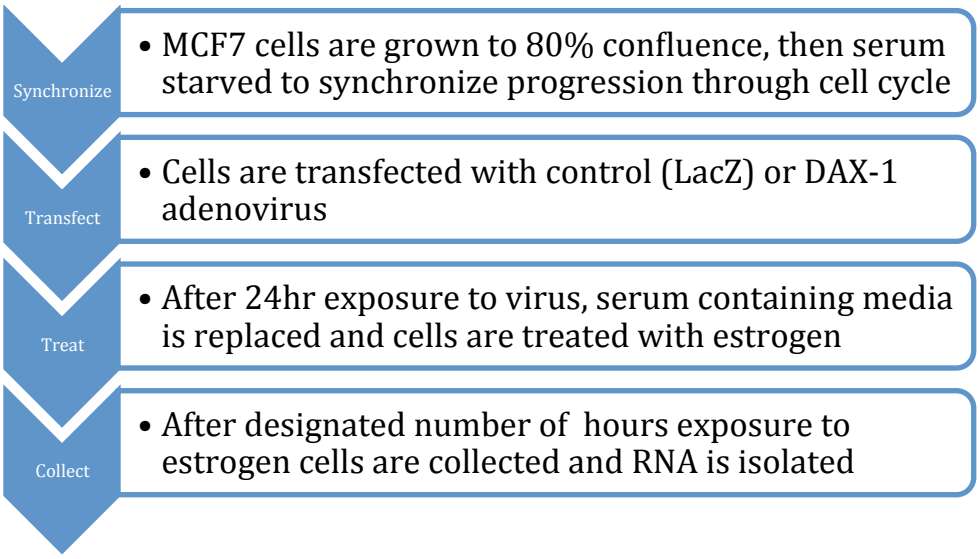

Figure 2-2 Viral transfection workflow.

is required to propel cells from G1 to S phase. Reducing Cyclin D1 expression through an increase in DAX-1 level slowed proliferation of the MCF7 cells.

To help confirm that the changes observed were due to repression of ERα by DAX-1, the proliferation assay was repeated in triple negative (ER, PR, and Her2 negative) breast cancer cell line (MDA-MB-231) that is epidermal growth factor (EGF) positive. The cells were transfected as before and treated with EGF for up to 120 hours. Some decrease in proliferation was observed in the DAX-1 treated cells, however the repression was much less striking compared to the ER positive MCF7 cells and cells did not regress beyond the starting number as was seen with the MCF7 cells (Figure 2-5 b). These findings help to support that the repression of proliferation seen in the MCF7 cells is largely due to DAX-1 inhibition of ERα activity. Without ERα, DAX-1 has some effect on proliferation, but not to the same level seen in the ERα positive MCF7 cells.

Expression of DAX-1 in human breast adenocarcinoma cells (MCF7) by plasmid transfection.

To confirm the data previously observed in the MCF7 breast cancer cells using the adenoviral transfection technique, I utilized another non-viral transfection method. Since non-viral transfection would later be used in RNA interference experiments, I used the same method for transfection of a plasmid containing the full-length wild-type DAX-1gene. Transfection of siRNAs required the use of lipid transfection, therefore the same transfection reagent was used to transfect DAX-1 and empty vector control plasmids. This would allow transfection conditions to be as similar as possible so that results could be more accurately compared between these two sets of experiments.

For these experiments cells were transfected with either an empty plasmid (vehicle control) or plasmid containing wild-type DAX-1 DNA sequence. MCF7 breast cancer cells were

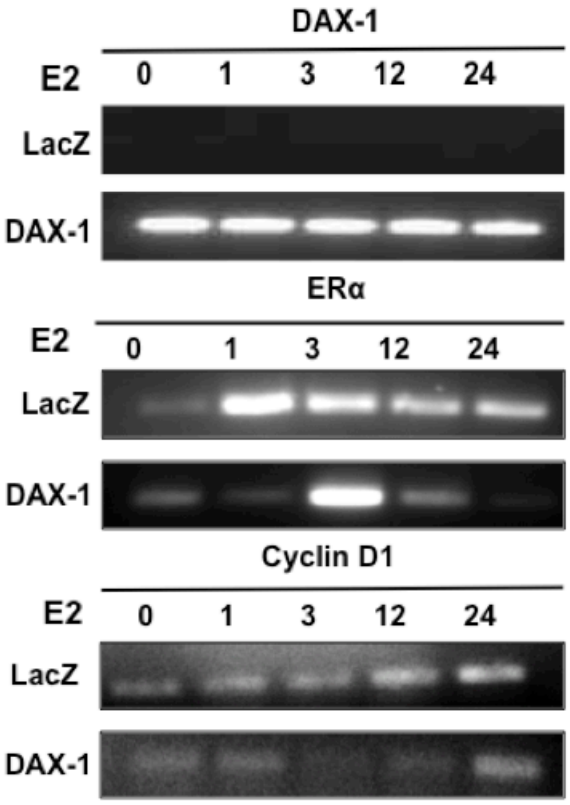

Figure 2-3. PCR expression results following viral infection of DAX-1 into MCF7 cells.
MCF7 cells were infected with LacZ (control) or DAX-1 containing adenovirus and treated with estrogen for up to 24 hours.
DAX-1: DAX-1 cDNA level is increased. Confirmation of transfection, DAX-1 is detectable only in DAX-1 treated cells.
ERα: ERα cDNA level is decreased with DAX-1 expression compared to LacZ control
Cyclin D1: Cyclin D1 cDNA level is decreased with DAX-1 expression compared to LacZ control.

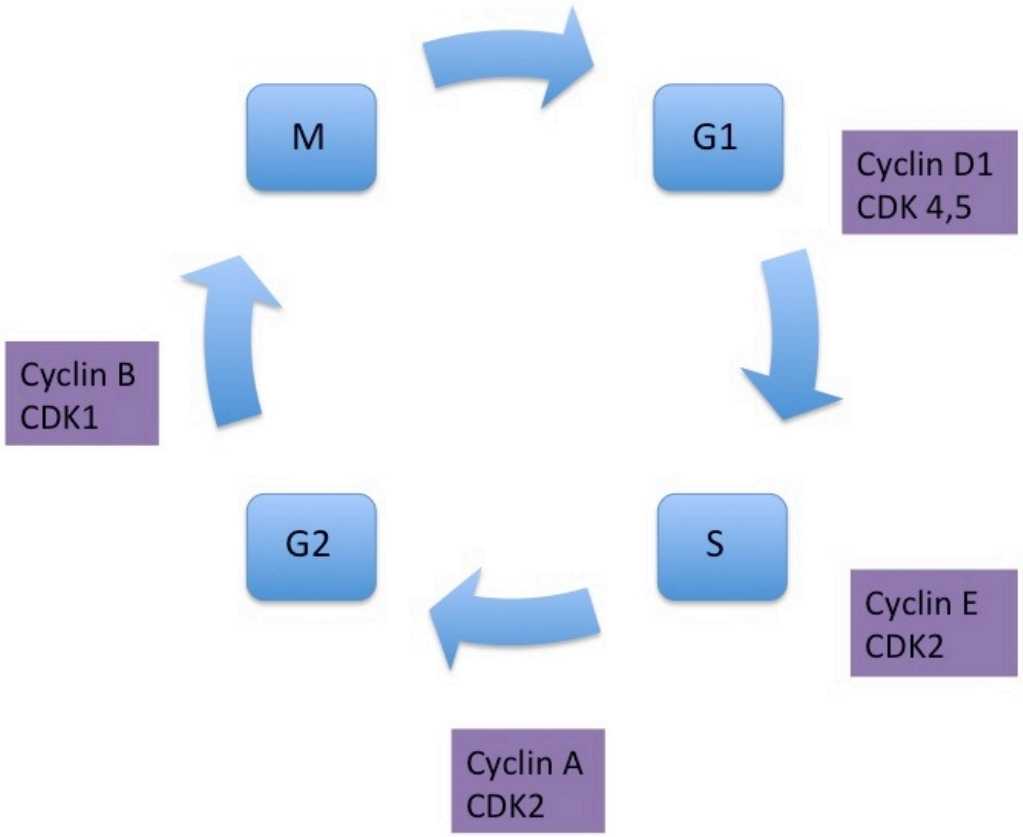

Figure 2-4. Cell cycle with cyclins.
Movement through the cell cycle depends on the presence of cyclins, which work together with their specific kinase, or CDKs. Each phase of the cell cycle is mediated by different cyclins/CDK combinations. Cyclin D drives progression through G1 and into S phase. Cyclin E mediates the shift from G1 to S phase. Cyclin A drives progression through S phase and Cyclin B mediates the shift from G2 into the mitotic phase. (Image taken from: S. L. Forsburg, UCSD)

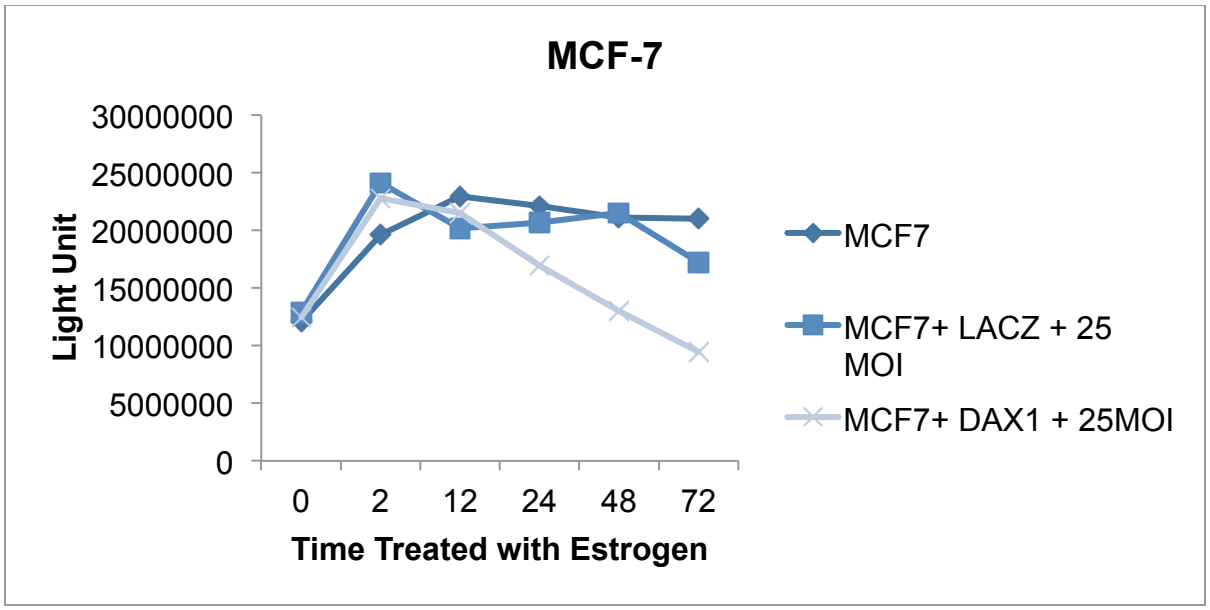

Figure 2-5a MCF7 ER positive cell proliferation assay.
MCF7 cells were left untreated or infected with either control (LacZ) or DAX-1 adenovirus and treated with E2 for up to 72 hours. DAX-1 infected cells had slower rate of growth and proliferation. DAX-1 treated cells regress beyond starting number of cells.

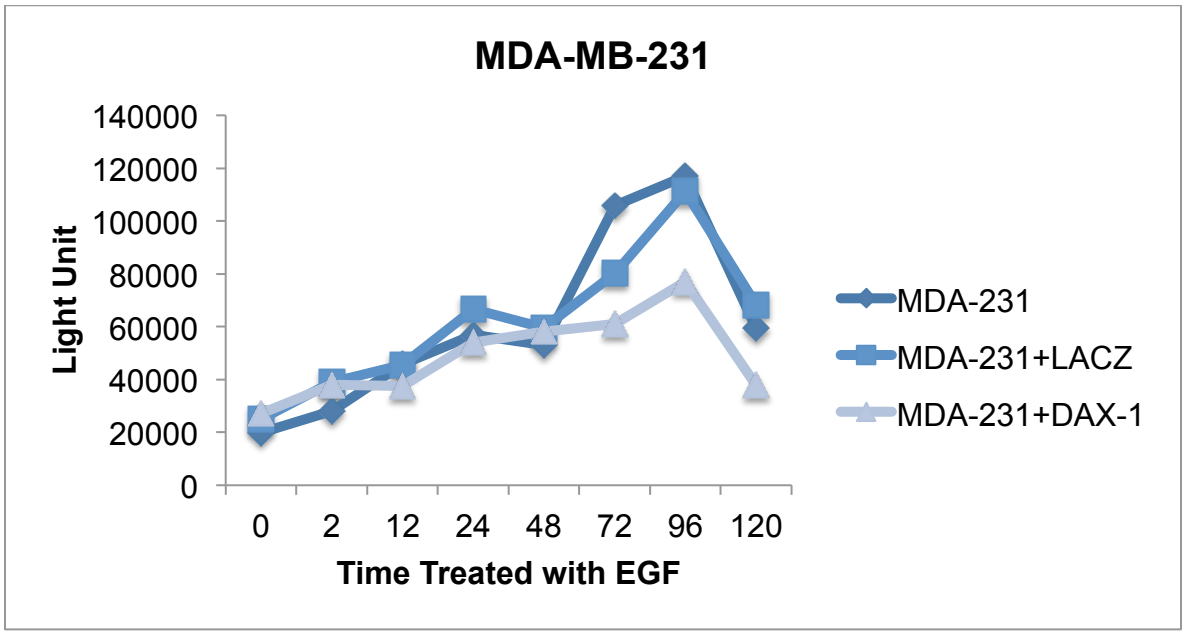

Figure 2-5b MDA-MB-231 ER negative cell proliferation assay.
Cells were left untreated or infetced with either control (LacZ) or DAX-1 adenovirus and treated with EGF for up to 120 hours. DAX-1 infected cells had a somewhat slower rate of growth and proliferation, but cells did not regress as with MCF7 cells.

plated and reverse transfected. Following transfection, cells were incubated for 48 hours, collected, and prepped for either mRNA isolation or protein lysis.

Expression levels of GAPDH (control housekeeping gene), DAX-1, and Cyclin D1 were examined by PCR and western blot (Figure 2-6 a and b). Successful transfection was confirmed by detection of DAX-1. As shown in Figure 2-6, an increase in the amout of DAX-1 was observed in the cells transfected with wild-type DAX-1 when compared to the untreated or empty vector control cells (lanes 1-3). When the amount of DAX-1 was increased, a significant decrease in the amount of Cyclin D1 was detected by standard PCR. This was confirmed by western blot, where the amount of Cyclin D1 protein was decreased upon DAX-1 introduction into cells. Quantitative PCR was performed to measure the change in expression of these two gene targets as well as estrogen receptor alpha (ERα). Using GAPDH as a reference, a 4.8 fold upregulation in the amount of DAX-1 cDNA ($p= .007$) and a 7.9 fold downregulation in the amount of Cyclin D1 cDNA ($p= .004$) was detected (Figure 2-7) upon DAX-1 introduction into MCF7 cells.

To determine if the decrease in Cyclin D1 observed had any effect on proliferation of the MCF7 cells, downstream proliferation targets were analyzed. Three specific S phase genes were chosen; Ki-67, MCM7, and TOP2A. Ki-67 is a nonhistone nuclear antigen and a classic proliferation marker. Proliferating cells have higher levels of Ki-67 than do cells that are in arrest or quiescent. Minichromosomal maintance complex component 7 (MCM7) is a protein that is essential for initiating genome replication and is involved in the formation of replication forks. Topoisomerase II alpha (TOP2A) is an enzyme that helps to change topological states of DNA during replication. TOP2A is involved in chromatid condensation, separation, and creating nicks

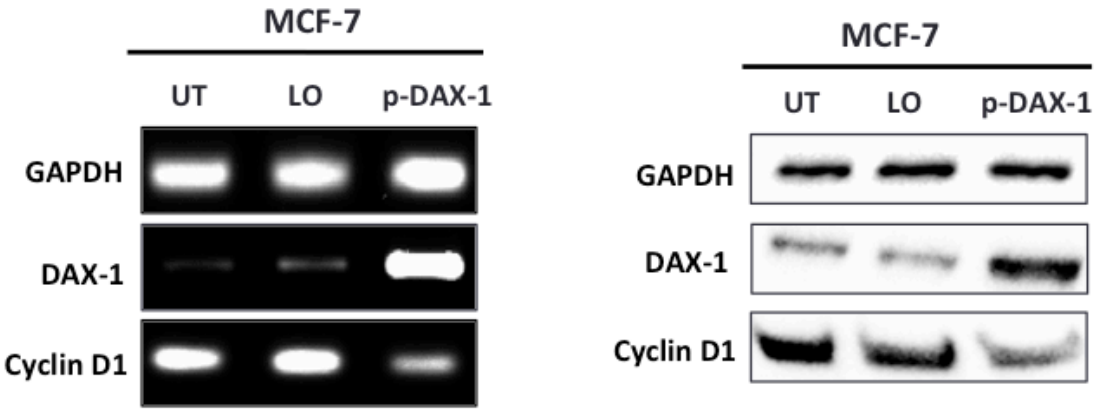

Figure 2-6 Target gene cDNA and protein levels in DAX-1 transfected MCF7 cells. cDNA (left) and protein (right) levels of GAPDH (control), DAX-1, and Cyclin D1 for transfected MCF7 breast cancer cells. When DAX-1 is expressed in MCF7 cells Cyclin D1 expression levels decrease. UT: untreated, LO: lipid transfection reagent only, p-DAX-1: WT DAX-1 plasmid.

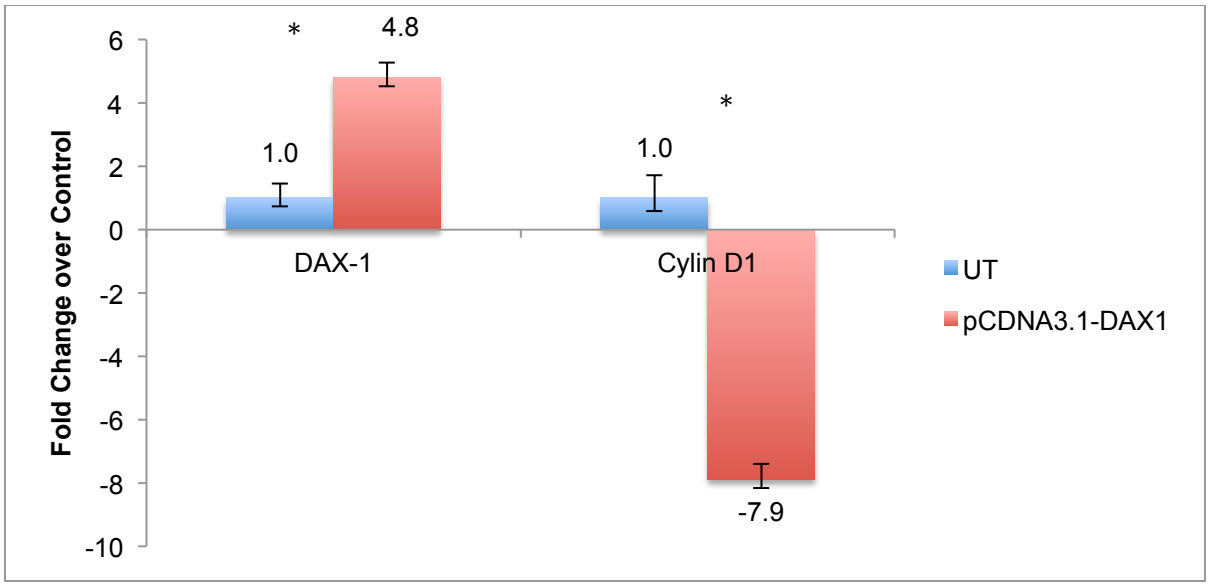

Figure 2-7 qPCR expression of DAX-1 and Cyclin D1 for DAX-1 transfected MCF7 cells. Increased DAX-1 expression by transfection of WT DAX-1 (pCDNA3.1-DAX1) results in a reduction in Cyclin D1 expression level when compared to untreated cell (UT).
$P<0.05$ *

in the DNA to help relieve torsional stress during DNA synthesis. These genes were chosen because they code for proteins that function and are increased during DNA sythesis.

Since DAX-1 has been shown to cause a reduction in Cyclin D1 levels, we hypothesize that fewer cells would be moving from G1 into S phase and undergoing DNA synthesis.

Results from qPCR data show a decrease in the three S phase genes upon DAX-1 treatment compared to untreated or vehicle control cells (Figure 2-8). Decreases in MCM7 and TOP2A were found to be statistically significant, $p = .05$ and $p = .03$ respectively. This data indicates that reduction of Cyclin D1 via DAX-1 repression of ERα caused cells to remain in G1 phase rather than progress to S phase, and as a result have a lower level of expression of the three S phase markers.

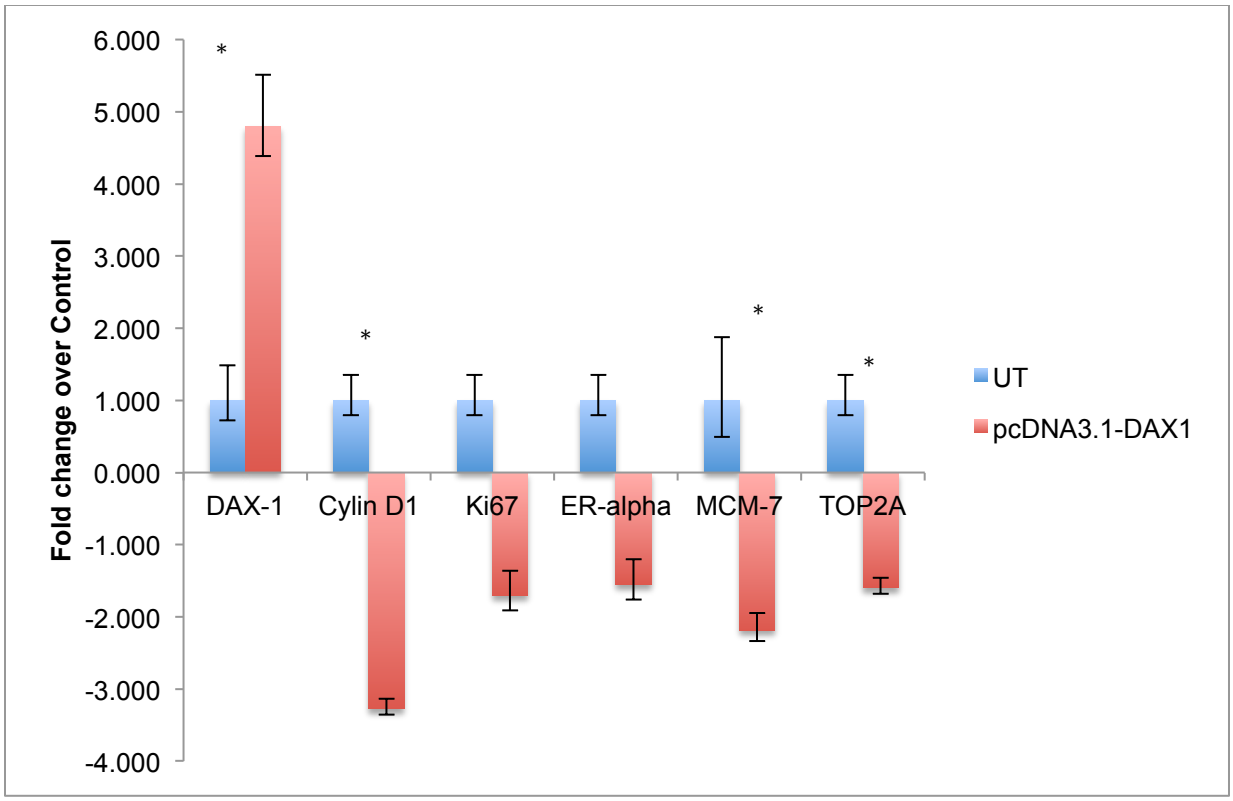

Figure 2-8 qPCR analysis of proliferation gene targets.
qPCR expression for MCF7 breast cancer cells untreated (UT) or WT DAX-1 plasmid (pcDNA3.1-DAX1). Increased DAX-1 expression (4.8 fold) caused a decrease in expression of Cyclin D1 (-3.3 fold), Ki-67 (-1.7 fold), ERα (-1.56 fold), MCM7 (-2.2 fold), and TOP2A (-1.6 fold). $P<0.05$ *

Knockdown of DAX-1 in human epithelial breast cells (MCF10A) by siRNA transfection.

Following detection of the anti-proliferative effects of expressing DAX-1 in the MCF7 breast cancer cells, I wished to address whether knockdown of DAX-1 expression via RNA interference (RNAi) in normal breast cells would give the opposite effect. A combination of three DAX-1 targeting small interfering RNAs (Life Technologies) was used to reduce expression of DAX-1. This technique takes advantage of an intrinsic molecular mechanism that allows for the specific targeting of an mRNA within the cell. RNAi results in a decrease in the number of transcripts present for the gene being targeted. Reducing the number of mRNA transcripts leads to decreased protein expression of the targeted gene. Using siRNA targeted towards DAX-1 provided a means to analyze downstream targets affected by the presence or reduction of DAX-1.

Normal human epithelial breast cells (MCF10A) were used as the model for these experiments as these cells are ER negative, but express DAX-1. Cells were plated and reverse transfected with either the pool of three DAX-1 targeting siRNAs or a control siRNA. Cells were collected after 48 hours of incubation and either mRNA isolation or whole cell protein lysate was prepared. Samples were analyzed by standard PCR, qPCR, and western blot for GAPDH (control), DAX-1, and Cyclin D1 expression (Figure 2-9). Knockdown of DAX-1 was confirmed visually with PCR and western blot as well as quantitatively by qPCR (Figure 2-10). When compared with the GAPDH control, a range from 4 to 8-fold decrease in DAX-1 levels was observed following treatment with DAX-1 targeting siRNA.

Once knockdown had been confirmed, Cyclin D1 levels were analyzed by PCR, qPCR, and western blot. As hypothesized, Cyclin D1 levels increased when the DAX-1 level was

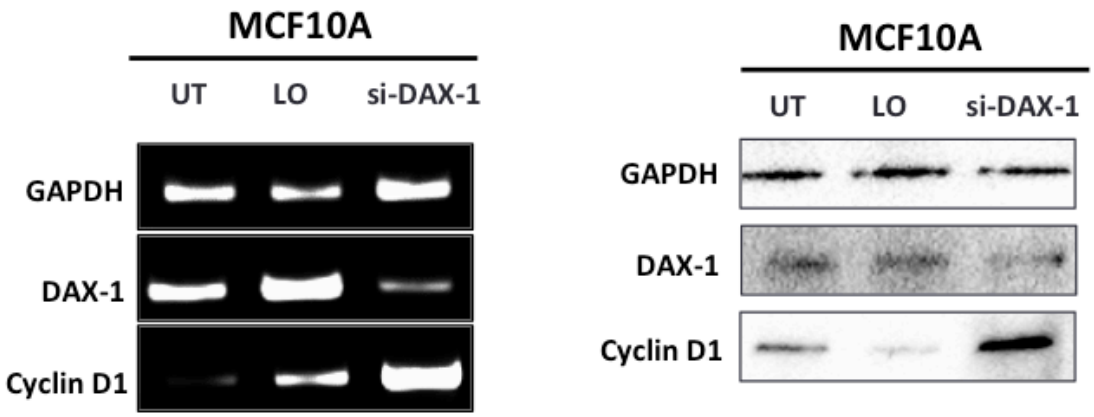

Figure 2-9 cDNA and protein levels following DAX-1 knockdown in MCF10A cells. cDNA (left) and protein (right) levels of GAPDH (control), DAX-1, and Cyclin D1 for siRNA transfected MCF10A normal breast cells. UT: untreated, LO: lipid transfection reagent only, si-DAX-1: set of three DAX-1 targeting siRNAs. When DAX-1 expression levels decrease, Cyclin D1 expression levels were shown to increase.

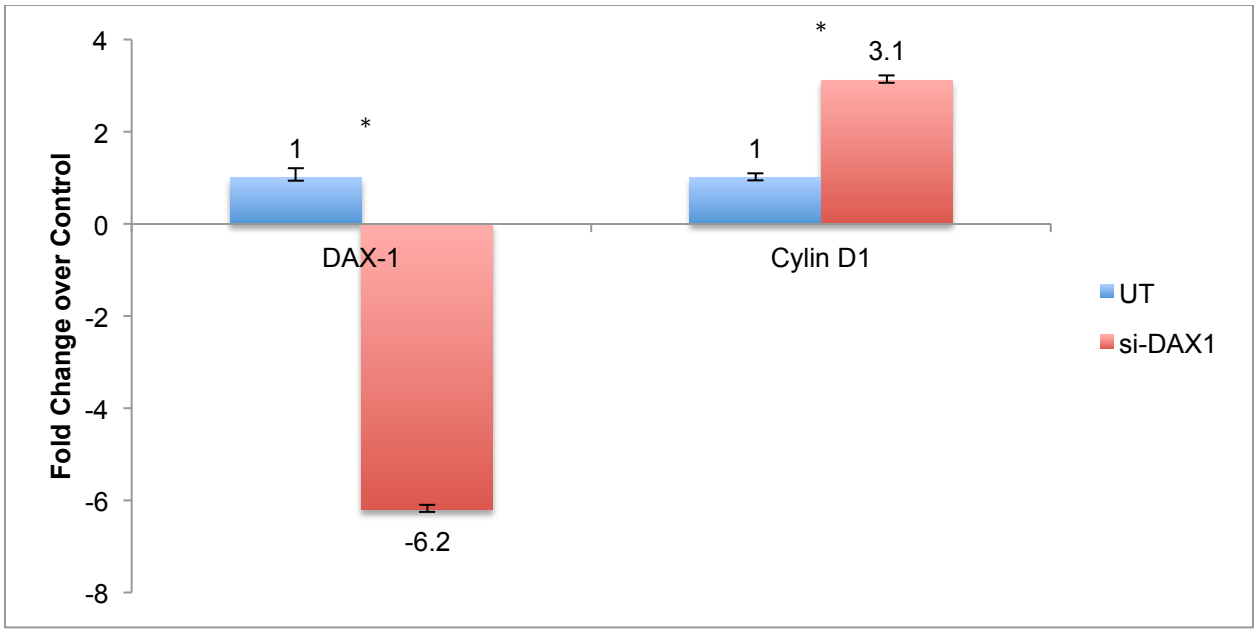

Figure 2-10 qPCR analysis of DAX-1 and Cyclin D1 following DAX-1 knockdown in MCF10A cells.
When DAX-1 expression level is reduced by siRNAs, Cyclin D1 expression levels increase. P<0.05 *

reduced (Figure 2-9 and 2-10). It was found by qPCR that DAX-1 decreased by a 6.2 fold-change (p= .005) and Cyclin D1 increased by a 3.1 fold-change (p= 0.002) when compared to untreated cells. S phase proliferation markers Ki67, MCM7, and TOP2A were analyzed by qPCR and were found to be significantly increased when compared to untreated and control cells (Figure 2-11). These results confirm the role of DAX-1 in slowing proliferation by repression of Cyclin D1 gene expression.

Cell cycle analysis of DAX-1 transfected MCF7 cells and DAX-1 knockdown MCF10A cells.

Cell cycle analysis is a way to determine what stage of the cell cycle a population of cells is in using propidium iodide (PI) staining of DNA (Figure 2-12). The amount of staining makes it possible to differentiate between cells in G0/G1, S phase, and G2/M phase. Cells in G2/M phase will have twice the amount of DNA as cells in G0/G1 and therefore twice the amount of signal from PI staining.

MCF7 breast cancer cells were transfected with either empty vector (plasmid only control) or a plasmid containing wild-type DAX-1. Concurrently, MCF10A normal breast cells were transfected with non-targeting control or DAX-1 targeting siRNAs. In both cases cells were incubated for 48 hours and collected. Collected cells were permeablized over-night with ethanol, stained with PI, and analyzed by flow cytometry. In the MCF7 breast cancer cells, there was a shift in the cells transfected with the DAX-1 plasmid. Specifically, more cells were in G0/G1 compared with the untreated or vehicle control transfected cells (Figure 2-13a). In the untreated cells and vehicle control cells, 30% and 30.2% respectively of the total cells were in G0/G1 phase, whereas in the DAX-1 transfected cells 40.3% of cells were in G0/G1 (Figure 2-13b).

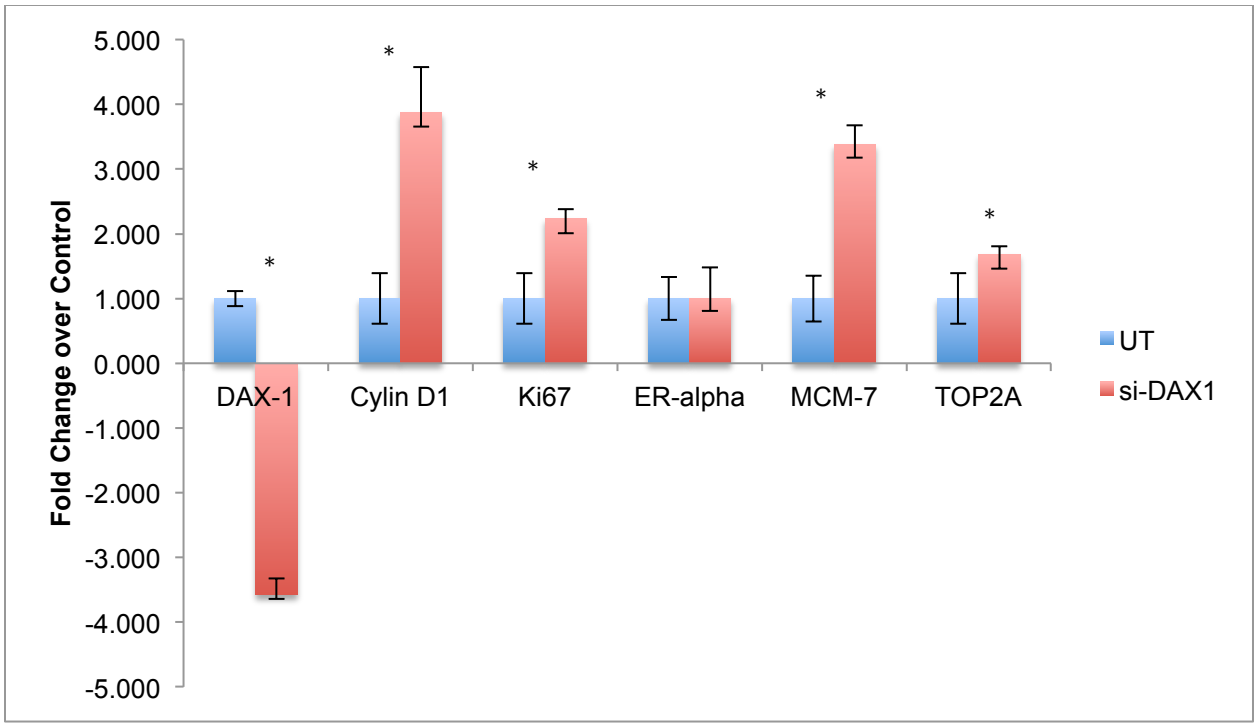

Figure 2-11 qPCR analysis of proliferation target genes.
qPCR expression for MCF10A normal breast cells that were either untreated (UT) or transfected with a set of three DAX-1 targeting siRNAs (si-DAX-1). DAX-1 knockdown (-3.6 fold) caused an increase in Cyclin D1 (3.9 fold) , Ki-67 (2.2 fold), MCM7 (3.4 fold), and TOP2A (1.7 fold). MCF10A cells are ER negative, therefore ER levels did not change when DAX-1 was knocked down by siRNA.
$P<0.05$ *

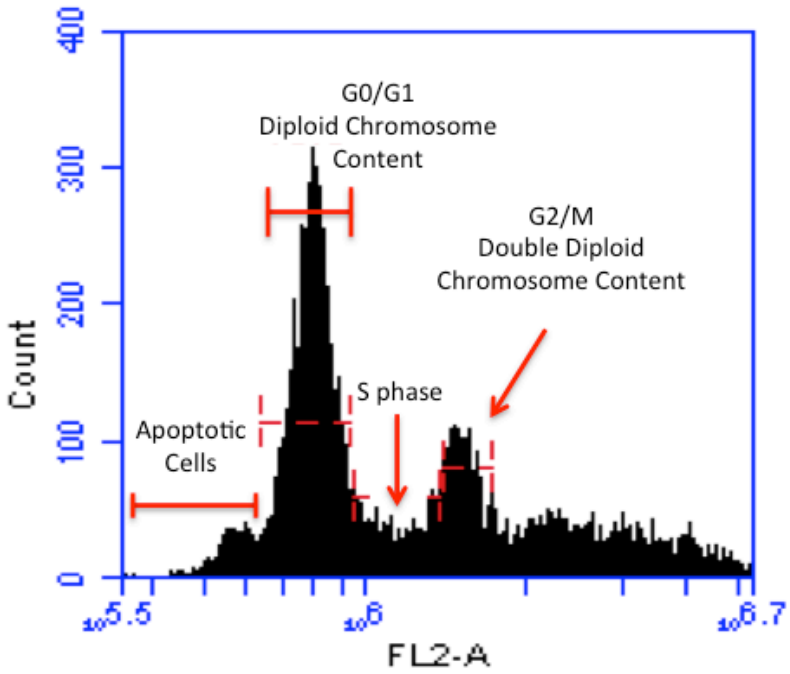

Figure 2-12 Cell cycle analysis diagram.
Peaks on histogram represent different stages of the cell cycle. Apoptotic cells are represented by the initial segment of the histogram, the first peak represents cells in G0/G1 (diploid chromosome content), the valley between peak one and two are cells in S-phase (somewhere between diploid and double diploid chromosome content), and the second peak represents cells in G2/M phase (double diploid chromosome content, ready to divide).

In the normal breast MCF10A cells there was a shift in the opposite direction when DAX-1 was knocked down by siRNA (Figure 2-14a). Untreated and non-targeting control siRNA treated samples had 51.1% and 47.7% of cells in G0/G1 compared to 42.5% of cells in G0/G1 for the DAX-1 knockdown cells (Figure 2-14b). These data help to support the hypothesis that DAX-1 functions as a repressor of growth and slows progression through the cell cycle. Not only is DAX-1 reducing the amount of Cyclin D1, but this reduction has downstream effects on both S phase genes as well as the rate of cells moving through the cell cycle as demonstrated by cell cycle analysis.

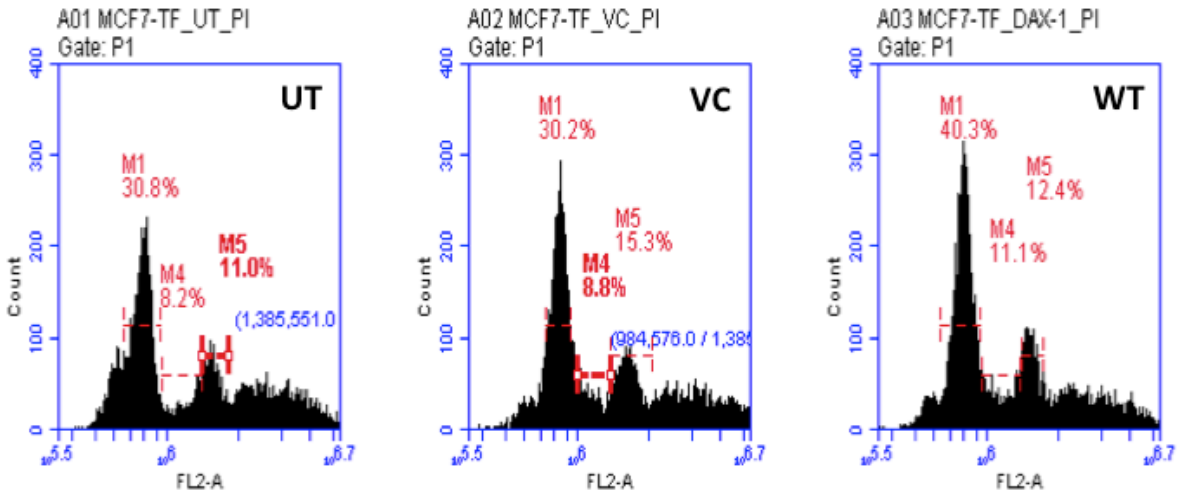

Figure 2-13a Cell cycle analysis for transfected MCF7 cells.
First peak in histogram represents proportion of cells in G0/G1 phase of cell cycle, second peak represents cells in G2/M phase of cell cycle. A greater proportion of cells transfected with DAX-1 were found in G0/G1 compared to untreated and control cells.
UT: untreated VC: vehicle control WT: wild-type DAX-1.

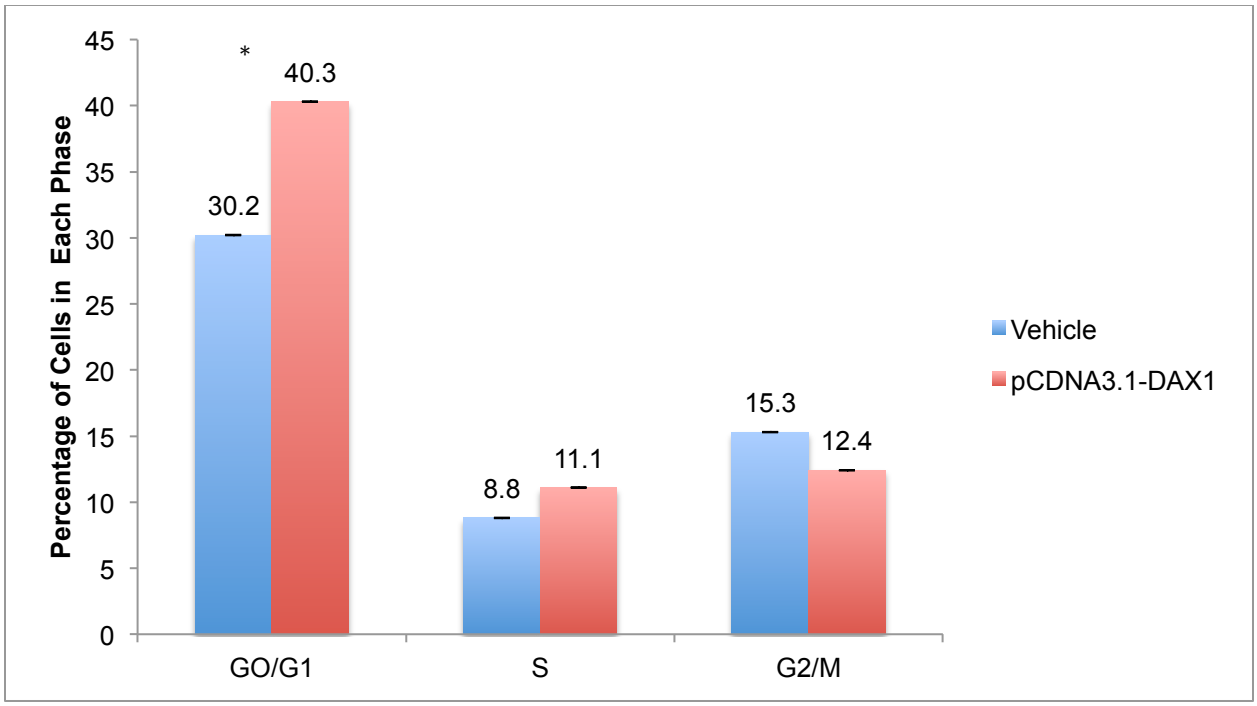

Figure 2-13b Quantification of cells in each phase of the cell cycle after transfection with DAX-1.
G0/G1 phase: Vehicle: 30.2% Wild-type DAX-1(pCDNA3.1-DAX1): 40.3%, S phase: Vehicle: 8.8% Wild-type DAX-1(pCDNA3.1-DAX1): 11.1%, G2/M phase: Vehicle:15.3% Wild-type DAX-1(pCDNA3.1-DAX1): 12.4%
Expression of DAX-1 leads to a greater percentage of cells remaining in G0/G1.
$P<0.05$ *

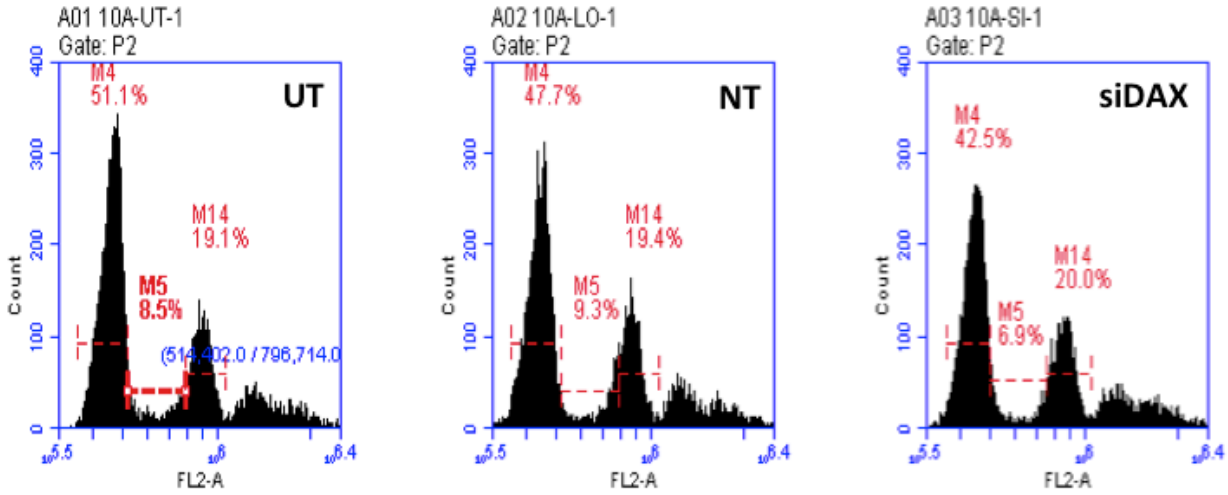

Figure 2-14a Cell cycle analysis of DAX-1 knockdown MCF10A cells.
First peak in histogram represents proportion of cells in G0/G1 phase of cell cycle, second peak represents cells in G2/M phase of cell cycle. DAX-1 knockdown cells (SI) have fewer cells in G0/G1 compared to untreated and control cells.
UT: untreated NT: non-targeting control siRNA siDAX: DAX-1 targeting siRNA.

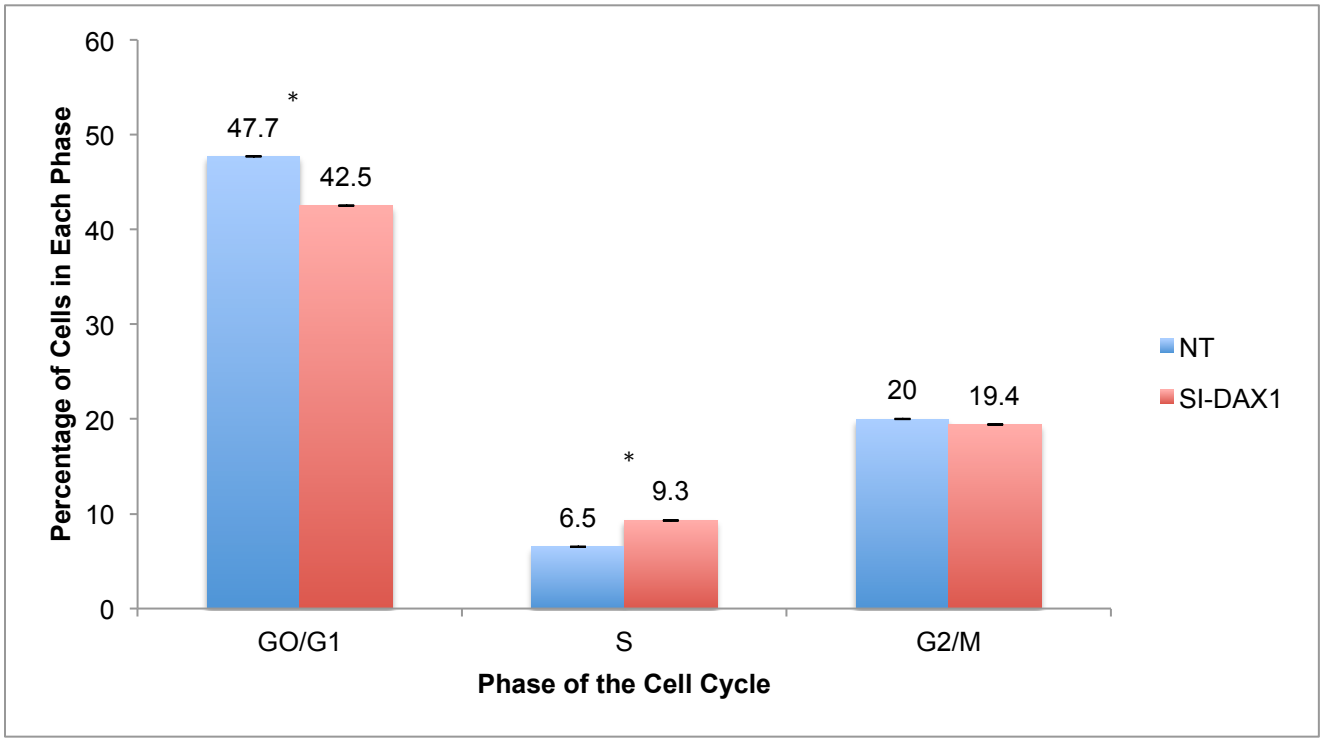

Figure 2-14b Quantification of cells in each phase of the cell cycle.
G0/G1 phase: Non-targeting siRNA control (si-NT): 47.7% DAX-1 targeting siRNA (si-DAX-1): 42.5%, S phase: Non-targeting siRNA control (si-NT): 9.3% DAX-1 targeting siRNA (si-DAX-1): 6.5%, G2/M phase: Non-targeting siRNA control (si-NT): 19.4% DAX-1 targeting siRNA (si-DAX-1): 20.0%
Knockdown of DAX-1 leads to fewer cells in G0/G1 and an increase of cells entering the cell cycle.
$P<0.05$ *

Chapter 2: Discussion and Future Directions

DAX-1 has been shown to act as a repressor of transcriptional activity for several nuclear hormone receptors [18, 40, 45]. This research aimed to explore known DAX-1 target genes, such as the NHR estrogen receptor alpha and its gene target Cyclin D1, as well as to identify additional proliferation targets affected by DAX-1 expression. By examining the effects of increasing DAX-1 expression in DAX-1 deficient cells as well as reducing expression of DAX-1 by siRNA knockdown in DAX-1 positive cells, it was determined that DAX-1 plays an important role in moderating proliferation. It is thought that DAX-1 exerts its repressive activity primarily through transcriptional inhibition of ERα. Repression of ERα prevents transcription of Cyclin D1, thereby preventing cells from transitioning into the G1 phase of the cell cycle. This was observed both by gene expression data as well as by proliferation assay and cell cycle analysis. A decrease in expression of three proliferation genes, Ki-67, MCM7, and TOP2A was observed in cells transfected with a DAX-1 expression plasmid. These three genes are not believed to be direct targets of DAX-1, rather their reduced expression is likely a consequence of DAX-1 inhibited progression through G1 phase of the cell cycle. Ki-67, MCM7, and TOP2A are markers connected with later stages of the cell cycle, therefore are not expressed when DAX-1 is present and causes a reduction in cell cycle progression.

Support of the expression data for DAX-1 transfected cells was reinforced by a viability proliferation assay demonstrating that MCF7 DAX-1 deficient cells transfected with a DAX-1 expression plasmid had reduced proliferation compared to untreated cells. Cells transfected with DAX-1 even regressed beyond the starting number of cells, indicating that DAX-1 may also play

some role in promoting apoptosis. Experiments exploring the possible role of DAX-1 in promoting apoptosis are currently being researched in the Tzagarakis-Foster lab.

From the results observed in the DAX-1 transfection experiments, it was hypothesized that knockdown of DAX-1 in DAX-1 positive MCF10A cells would lead to the opposite effect and an increase of proliferative gene targets would result. This hypothesis was supported by expression data. Expression levels of Cyclin D1, Ki-67, MCM7, and TOP2A were all found to increase when DAX-1 was knocked down in MCF10A cells. This cell line is ERα negative, indicating that aside from this known target, DAX-1 must be able to act through another gene target. Determination of this mechanism of repression is the subject of ongoing research in the Tzagarakis-Foster Lab and may tie in to the hypothesis that DAX-1 is not only involved in proliferation, but that it may also play a role in apoptosis.

Chapter 3: Determining the SUMOylation status and effects of SUMOylation on DAX-1

Chapter 3: Introduction

SUMOylation involves the post-translational addition of one or more SUMO (small ubiquitin-related modifier) peptides to target proteins. The SUMO gene (*SMT3*) was first discovered in the mid 1990's and was originally identified in *Saccharomyces cerevisae.* SUMO was later observed as a binding partner for the human proteins RAD51, RAD52, and FAS [46-48]. RAD51 and RAD52 are important proteins for the repair of double stranded breaks in DNA, whereas FAS is known as the death receptor and plays an important role in the extrinsic apoptosis pathway. The interaction that solidified SUMO as an interesting and important protein was the discovery of SUMO covalently attached to Ran GTPase-activating protein (RanGAP1)[49]. This was of particular significance because unmodified RanGAP1 is only found in the cytosol, whereas SUMOylated RanGAP1 is found in the nucleus [49, 50]. This discovery helped to define two key characteristics of SUMO and the effects of SUMOylation: SUMOylation is a reversible and dynamic post-translational modification, and SUMOylation can alter the localization of proteins by changing protein interactions [51].

SUMO proteins are expressed in all eukaryotes. Although some organisms have only a single SUMO protein, humans have been found to express four different SUMO proteins (SUMO 1-4) [52]. In humans SUMO1-SUMO3 are expressed ubiquitously, wereas SUMO4 is expressed more selectively in the lymph nodes, spleen, and kidneys [53]. The four SUMO proteins are approximately 10 kDa in size and though they resemble ubiquitins in structure, they share only 20% amino acid sequence identity [51]. SUMO2 and SUMO3 are very similar at 97% sequence identity, but share only 50% amino acid sequence identity with SUMO1 [54]. The functions of SUMOs appear to be distinct as the different types of SUMO are often conjugated to different proteins *in vivo* [55, 56]. The role of SUMO4 is still unclear [53].

SUMOylation occurs at specific consensus binding sites within a target protein. The SUMO-acceptor site has been shown to be ΨKxE, where Ψ is a branched hydrophobic amino acid, K is a lysine reside, x is any amino acid, and E is a glutamic acid [57]. The lysine residue is the actual site of attachment of the SUMO protein.

In the past decade the enzymes involved in SUMOylation have been identified, as have numerous SUMO targets, many of which are nuclear proteins. The reversible mechanism of SUMOylation involves three classes of enzymes: E1 activating enzymes, E2 conjugating enzymes, and E3 ligating enzymes. Mature SUMO proteins are first activated with an E1 activating enzyme heterodimer AOS1-UBA2. This reaction results in a thioester bond formation between the C-terminal carboxyl group of SUMO and the catalytic cysteine residue of UBA2 [58, 59]. After activation, SUMO is conjugated to E2 activating enzyme UBC9 via another thioester bond with a cysteine residue on UBC9 [60, 61]. SUMO is then ligated to target proteins via an isopeptide bond formed between the C-terminal glycine on SUMO and a lysine residue of the target protein [62, 63]. This ligation step is carried out by E3 ligases that transfer SUMO from UBC9 onto the target. There are a number of ligases that can carry out this final step in the SUMOylation process, including members of the protein inhibitor of activated STAT (PIAS) family of enzymes [62-64]. Most often a single SUMO protein is added to a target, however polySUMO chains have been seen with SUMO2/3 [61].

Removal of SUMOylation from a target protein occurs via a number of different proteases. Three different isopeptidases observed to carry out deSUMOylation are the sentrin-specific proteases (SENP1-3, SENP5-7), SUMO-specific protease (SUSP1), and ubiquitin-like protease (Ulp) [51, 57]. The SENP family of enzymes is responsible not only for the cleavage of SUMO from target proteins, but also for the hydrolysis of newly synthesized SUMO proteins to

their mature form [65]. SUMO proteins are synthesized with a variable C-terminal stretch of 2-11 amino acids that follows a conserved glycine-glycine motif; this is the region that is cleaved to form the mature SUMO protein [54]. The C-terminal glycine-glycine region is where SUMO attachment to lysine residues in the target protein occurs.

SUMOylation has been identified on many protein targets including transcription factors, cofactors, and coregulators [57]. The addition of SUMO to transcription factors tends to result in a decrease in transcriptional activity and an overall reduction in gene expression [66]. SUMOylation sites have been identified on a number of nuclear hormone receptors including progesterone receptor, estrogen receptor, androgen receptor, and steroidogenic factor 1 (SF-1) [67-69]. SF-1, a close relative of DAX-1, is responsible for normal endocrine tissue development and regulation of reproductive and stress endocrine signaling axes. When SF-1 SUMOylation sites were eliminated by knock-in mouse models, mice developed smaller adrenal glands and had numerous abnormalities in development of the gonads, all of which led to infertility in both males and females [69]. These knock-in SUMO mutants also exhibited changes in normal hedgehog signaling patterns. In wild-type mice, desert hedgehog (*Dhh*) expression is present in the testes and sonic hedgehog (*Shh*) is absent. However in the SUMO mutant mice, *Shh* expression was detectable and *Dhh* expression was reduced [69]. The striking changes observed with mutation of SUMO sites within SF-1 led to the hypothesis that DAX-1 may also be SUMOylated and that mutation of DAX-1 SUMO sites may lead to changes in activity or function of DAX-1.

In my research, I have determined the SUMOylation status of DAX-1 and explored the effects of SUMOylation on DAX-1 by mutating putative SUMO sites within the DAX-1 gene. Wild-type and DAX-1 SUMO mutants were transfected into MCF7 cells to compare differential

expression of target genes. Effects of SUMOylation on cell cycle progression and apoptosis were also examined. By determining the SUMOylation status and effects of SUMOylation on DAX-1, we hope to gain a better understanding of how this post-translational modification alters the function of DAX-1.

Chapter 3: Materials and Methods

Cell Culture

All cell lines were routinely passaged, cultured, and maintained at 37° C in a humidified 5% CO_2 tissue culture incubator as described in Chapter 2. MCF7 human breast cancer cells and MCF10A normal breast cells were cultured as described in Chapter 2.

SW13 human adrenal carcinoma cells, MDA-MB-231 human triple negative breast cancer cells, and A549 human lung carcinoma cells were cultured in Dulbecco's modified eagle medium (DMEM) and Ham's F12 (1:1) with phenol red and supplemented with 10% Fetal Bovine Serum (ATCC, Manassas, VA), 1% L-Glutamine (Invitrogen, Carlsbad, CA), 1% NEAA (Invitrogen, Carlsbad, CA), (1% Penicillin/Steptomycin (Invitrogen, Carlsbad, CA), and 1% Fungizone (Invitrogen, Carlsbad, CA).

DNA Isolation

Plasmid DNA was isolated using PureYield Plasmid Miniprep System (Promega, Madison, WI) according to the manufacturer's instructions using a starting volume of 2 mL of bacterial culture. Purified DNA was measured using the NanoDrop 1000 Spectrophotometer (Thermo Scientific, Wilmington, DE) and sequenced (McLab, South San Francisco, CA) to confirm DNA sequences.

RNA Isolation and cDNA Synthesis

Total RNA was isolated using the RNeasy Mini Kit (Qiagen, Valencia, CA) as per the manufacturer's instruction, with the optional RNase-Free DNAse (Qiagen) step added to remove genomic DNA contamination. RNA was measured for concentration and purity using

the NanoDrop 1000 Spectrophotometer (Thermo Scientific, Wilmington, DE). High Capacity cDNA Reverse Transcription Kit (Applied Biosystems, Foster City, CA) was used to make cDNA with isolated RNA according to manufacturer's instructions. Thermocycling was carried out using MJ Mini Personal ThermoCycler (BioRad, Hercules, CA) with the following conditions.

	Step 1	**Step 2**	**Step 3**	**Step 4**
Temperature	25°C	37°C	85°C	4°C
Time	10 min	120 min	5 min	∞

Table 3-1 cDNA synthesis thermocycler conditions.

cDNA was then measured via NanoDrop, diluted, and normalized for subsequent PCR analysis.

Plasmid Transfection

pcDNA 3.1 plasmid (Life Technologies, Carlsbad, CA) containing no insert, wild-type DAX-1 or SUMO DAX-1 mutant DNA sequences were transfected into MCF7 cells seeded in six cell plates using a range of concentrations (1500-2000ng) of plasmid with 50µL of Lafectine RU50 transfection reagent (MednaBio, Burlingame, CA). Cells were incubated for 48 hours and then collected for total RNA isolation and whole cell protein lysate.

Protein Isolation

Whole cell protein lysate was collected following 24 or 48-hour treatments using either NP-40 or RIPA lysis buffer (Boston BioProducts, Worcester, MA) with Halt Protease Inhibitor (Thermo Fisher Scientific, Rockford, IL) added at a concentration of 1:100. Cells were collected from 6 well plates and centrifuged at 14,000 g for 5 minutes. Supernatant was removed and pelleted cells were resuspended in lysis buffer and incubated on ice for 15 minutes. Samples were

sonicated at an amplitude of 50 for two pulses of 30 seconds with a 40 second pause between pulses. The lysate was centrifuged at 14,000 g for 10 minutes to pellet insoluble materials and the supernatant was transferred to a new tube and stored at -70°C for future analysis.

Western Blot

Western blots were performed using the XCell II Blot Module (Invitrogen, Carlsbad, CA) according to the NuPAGE Novex Bis-Tris Protocol (Invitrogen, Carlsbad, CA) using 4X NuPAGE LDS sample loading buffer and 10X NuPAGE sample reducing agent. Samples were normalized using the Coomassie Plus Bradford Protein Assay (Thermo Fisher Scientific, Rockford, IL) and then combined with sample loading buffer and reducing-agent to a final volume of 30uL. Samples were electrophoresed through gradient 4-12% Bis-Tris SDS-PAGE gels for 45 minutes at 200V on the XCell II Blot Module. Protein was transferred from gel to PVDF membrane according to manufacturer's protocol using XCell II Blot Module with Blot apparatus. Blots were transferred at 25V for 1 hour. Membranes were then blocked at room temperature in 5% Blotto made in 1X Tris-Buffered Saline with 0.5% Tween 20 (TBST) for 1 hour with rocking at 150 RPM and incubated overnight at 4° C with primary antibody (listed below) made in 5% Blotto at 1:1000 dilution with rocking at 150 RPM.

Western blots were developed using the chemiluminescence Thermo Scientific Kit and analyzed using the BioRad GelDoc System (BioRad, Hercules, CA).

Protein	Species	Company
DAX-1 (K-17)	Rabbit polyclonal	Santa Cruz Biotech Santa Cruz, CA
DAX-1	Mouse monoclonal	Active Motif Carlsbad, CA
GAPDH	Mouse monoclonal	Santa Cruz Biotech Santa Cruz, CA
SUMO-1 (C9H1)	Rabbit monoclonal	Cell Signaling Technologies Danvers, MA
SUMO-2/3 (I8H8)	Rabbit monoclonal	Cell Signaling Technologies Danvers, MA

Table 3-2 Antibodies.

Standard PCR and qPCR

cDNA was synthesized from extracted mRNA and was used as template for standard PCR and qPCR. Samples for standard PCR were prepared using 11µL of 2X GoGreen (Promega, Madison, WI) or Taq 2X Master Mix (New England BioLabs, Ipswich, MA), 0.25µL of 10µM forward and reverse primers (listed in Table 3-4) , 12µL of dH2O, and 2µL cDNA. PCR was performed using MJ Mini Personal ThermoCycler (BioRad, Hercules, CA) using the protocol below with varying annealing temperatures.

Step	Temp	Time
Initial Denaturation	95°	4 minutes
30 Cycles: Denaturation Annealing Elongation	 95° 45-65° 72°	 30 sec 30 sec 30 sec
Final Extension	72°	4 minutes
Hold	4°	∞

Table 3-3 PCR thermocycler conditions.

Following PCR, samples were electrophoresed through a 1.5-2% 1X TAE agarose gel containing ethidium bromide. PCR products were visualized by ultraviolet light exposure using the BioRad GelDoc System (BioRad, Hercules, CA).

qPCR reactions were performed in triplicate using BioRad CFX96 Real-Time PCR system. qPCR reactions were prepared using 10.5 µL of SYBR Green Master Mix (Life Technologies, Carlsbad, CA), 0.25µL of 10µM forward and reverse primers (listed in table 2-5), 12µL of dH2O, and 2µL cDNA. GAPDH housekeeping gene was used as control and experimental genes were compared to GAPDH as a baseline. Fold-change values were calculated by comparing untreated and transfected samples. Error bars on qPCR results represent standard deviation (positive error) and standard error (negative error). Statistical significance of qPCR data is indicated on graphs by asterisks: $P<0.05$ * $P<0.01$ ** $P<0.005$ ***.

Gene Name	**Fwd Primer (5'-3')**	**Rev Primer (5'-3')**	**Annealing Temp**
GAPDH	ACA GCC GCA TCT TCT TGT GCA	GGG CTT GAC TGT GCC GTT GAA	58° C
DAX-1	GAC TCC AGT GGG GAA CTC AG	ATG ATG GGC CTG AAG AAC AG	57° C
CyclinD1	TAG CAC CTT GGA TGG GTA ATT	ATC GTG CGG CAT TGC GGC	59° C
ERα	CCA CCA ACC AGTT GCA CCA TT	GCG AGT CTC CTT GGC AGA TCC	54° C
Ki-67	ACA GAC CTC AAG AGC TTG CC	CCA GGG ATG CCT TCA ACT GT	57° C
MCM7	TGG CAC TGA AGG ACT ACG	CTG AGG CAG CAG CTC TTG TA	56° C

TOP2A	TGG GGT CCT GCC TGT TTA GT	TGT CTG GGC GGA GCA AAA TA	55° C

Table 3-4 PCR primers.

PCR Mutagenesis

DAX-1 SUMO mutants were constructed using the QuikChange Lightning Site-Directed Mutagnesis Kit (Agilent Technologies, La Jolla, CA). Primers were designed to mutate lysine residues at positions 249 and 362 within the DAX-1 amino acid sequence (Table 3-5). Mutagenesis primers and pcDNA 3.1 plasmid (Life Technologies, Carlsbad, CA) containing the wild-type DAX-1 sequence were used along with the QuikChange Lightning Site-Directed Mutagnesis Kit as per the manufacture's protocol. Following PCR mutagenesis, the resulting product was digested with methylation-specific restriction endonuclease Dpn1, allowing for the digestion of parental plasmid only. Nascent plasmids were transformed into XL10-Gold Ultracompetent bacterial cells, isolated colonies were grown overnight in LB with 10μg/mL ampicillin, then plasmid DNA was isolated (as described above in DNA isolation). Clones that contained the correct mutation were identified by DNA sequence analysis.

The SUMO double mutant was made using pcDNA K249A DAX-1 plasmid with K362A mutagenesis primers.

Mutation	**Fwd Primer 5'-3'**	**Rev Primer 5'-3'**
K249A	GCC GGT GGC GCT CGC GAG TCC ACA GGT	CGG CCA CCG CGA GCG CTC AGG TGT CCA C
K362A	TCC CAG GTC CAA GCC ATC GCG TGC TTT CTT TCC AAA TGC	GCA TTT GGA AAG AAA GCA CGC GAT GGC TTG GAC CTG GGA

Table 3-5 Mutagenesis primers.

Cell-Free Expression

Wild-type and SUMO mutant DAX-1 proteins were expressed from the pcDNA vector containing DAX-1 inserts using TNT T7 Quick Coupled Transcription/Translation System (Promega, Madison, WI). Protein was synthesized as per the manufacturer's protocol using 40µL TNT T7 Quick Master Mix, 1µL 1mM Methionine, 2µL template plasmid (1 µg total), and 7µL nuclease-free water. Reactions were incubated at 30° C for 90 minutes to complete synthesis.

In vitro SUMOylation

Wild-type and SUMO mutant DAX-1 proteins expressed *in vitro* (TNT T7 Quick Coupled Transcription /Translation System) were used as template with an *in vitro* SUMOylation Kit (Enzo Life Sciences, Farmingdale, NY). SUMOylation reactions for SUMO1, SUMO2, and SUMO3 were carried as per manufacturer's protocol using 2µL protein. Results were assayed by western blot using SUMO1 and SUMO2/3 antibodies provided with the kit. Blocking and antibody binding steps utilized 3% bovine serum albumen (BSA) in phosphate buffered saline with 0.5% Tween 20 (1X PBS-T).

Co-Immunoprecipitation (Co-IP)

To detect the presence of SUMOylation on DAX-1, Co-IP was carried out in several mammalian cell lines. Cells were collected and lysed as described previously (Protein Isolation). Whole cell lysates were mixed with Protein G Magnetic Beads (New England BioLabs, Ipswich, MA) to eliminate non-specific binding of protein to beads. Beads were removed from lysates and discarded after one hour incubation with rotation at 4° C. DAX-1 mouse primary antibody was added and incubated with rotation at 4° C overnight. Beads

were washed three times with 500µL RIPA lysis buffer (Boston BioProducts, Worcester, MA) with Halt Protease Inhibitor (Thermo Fisher Scientific, Rockford, IL) added at a concentration of 1:100. Washed beads were resuspended in 4X NuPAGE LDS sample loading buffer and 10X NuPAGE sample reducing agent and electrophoresed through a 4-12% gel. Proteins were transferred onto PVDF membranes and western blot analysis was carried out using SUMO 1, SUMO 2/3, and DAX-1 antibodies.

Cell Cycle Analysis

MCF7 cells were grown in 6 well plates and transfected with wild-type DAX-1 or SUMO mutant DAX-1 plasmids (previously described). Cells were collected and pelleted by centrifugation at 5,000 g for 5 minutes, resuspended and washed in 500µL PBS, and centrifuged at 5,000 g for 5 minutes. Supernatant was removed. Cells were resuspended in 50µL PBS, and mixed with 500µL of 100% ethanol. Cells were stored overnight at -20°C. Cells were centrifuged at 5,000 g for 5 minutes and supernatant was removed. Cells were resuspended with 100µL PI/RNase Staining Buffer (BD Pharmingen, San Diego, CA) and 10µL Propidium Iodide Staining Solution (BD Pharmingen, San Diego, CA) was added and incubated for 10 minutes before analysis by flow cytometry, using the BD Acurri C6 (BD Biosciences, San Jose, CA) flow cytometer. Cell cycle analysis samples were run in duplicate. Statistical significance calculated by using two tailed T-test comparing untreated and transfected groups. Data found to be statistically significant ($p < 0.05$) is indicated by asterisks.

Apoptosis Analysis

MCF7 cells were grown in 6 well plates and transfected with wild-type DAX-1 or SUMO mutant DAX-1 plasmids (previously described). Cells were collected and pelleted by centrifugation at 5,000 g for 5 minutes, resuspended and washed in 500µL PBS, and centrifuged at 5,000 g for 5 minutes. Supernatant was removed. Cells were resuspended with 100µL 1X binding buffer (10X solution contains 0.1 M Hepes pH 7.4, 1.4 M NaCl, 25 mM $CaCl_2$) and mixed with 10µL Propidium Iodide Staining Solution (BD Pharmingen, San Diego, CA) and 5µL FITC Annexin V (BD Pharmingen, San Diego, CA). Cells were incubated for 10 minutes before analysis by flow cytometry, using the BD Acurri C6 (BD Biosciences, San Jose, CA) flow cytometer. Apoptosis analysis samples were run in duplicate. Statistical significance calculated by using two tailed T-test comparing untreated and transfected groups. Data found to be statistically significant ($p < 0.05$) is indicated by asterisks.

Chapter 3: Results

Determination of DAX-1 SUMOylation Status

In order to determine the SUMOylation status of DAX-1, the predictive software, Abgent SUMOplot was used to analyze the amino acid sequence of DAX-1. The analysis revealed several putative sites with varying scores (Figure 3-1). This indicated that DAX-1 had a strong probability of being SUMOylated. In order to confirm DAX-1 was, in fact, SUMOylated in cells a co-immunoprecipitation (Co-IP) experiment was performed using several human cell lines, including normal and disease states (Figure 3-2). Whole cell lysates were collected from each cell line and incubated with a DAX-1 antibody overnight. Antibody and bound DAX-1 protein was isolated using magnetic protein G beads. The presence of SUMO-1 and SUMO-2/3 on immunoprecipitated DAX-1 was assayed by western blot. It was found that SUMOylated DAX-1 was present in all cell lines tested (Table 3-6). The different isoforms of SUMO were differentially expressed in the various cell lines. As seen in Figure 3-2, A549 cells had greater SUMO-2/3 levels than SUMO-1 levels when co-immunoprecipitated with DAX-1. SW13, MDA-MB-231, MCF7, and MCF10A cells had similar detection levels for both SUMO-1 and SUMO-2/3 when compared within the cell line, but had varying levels of SUMOylation between the cell lines overall. As a control, a western blot to confirm the presence of DAX-1 was included. This data demonstrates that in the cell lines examined, DAX-1 is SUMOylated.

Figure 3-1 DAX-1 amino acid sequence and protein map showing putative SUMOylation sites.

DAX-1 amino acid sequence with putative SUMOylation sites shown in red. Lysine residues at positions 249 and 362 were predicted as the highest probability sites for SUMOylation.
Below: DAX-1 protein map showing location of potential SUMO sites at K249 and K362.

Cell Line	Origin
A549	Lung Carcinoma
SW13	Adrenal Carcinoma
MDA-MB-231	Triple Negative Breast Cancer
MCF10A	Normal Mammary Epithelium
MCF7	Breast Adenocarcinoma

Table 3-6 Cell lines tested for SUMOylation of DAX-1 by Co-IP.
Five human cell lines were tested for the presence of SUMO proteins on immunoprecipitated DAX-1 from whole cell lysates. Four of the five cell lines tested were cancerous and one was normal tissue.

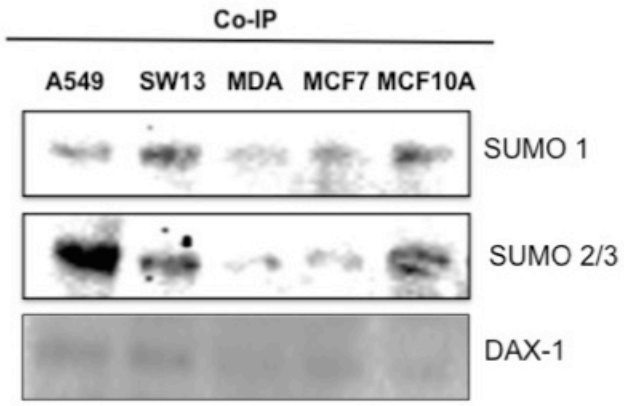

Figure 3-2 Co-IP of SUMO-1, SUMO-2/3, and DAX-1.
Five human cell lines listed in Table 3-6 were grown and collected as whole cell lysates. Lysates were immunoprecipitated with DAX-1 antibody and analyzed by western blot for the presence of SUMO-1, SUMO-2/3, and DAX-1 (control). Different cell types had varying amounts of each type of SUMO, but all were positive for the presence of SUMO.

Mutation of DAX-1 putative SUMO sites and in vitro SUMOylation.

Once confident that DAX-1 was a bona fide SUMOylation target and that it was SUMOylated in A549, SW13, MDA-MB-231, MCF7, and MCF10A cell lines, I wished to determine the effects of mutating the putative SUMO sites in the DAX-1 protein. The two potential SUMO sites with the highest probability scores were lysine 249 and lysine 362, which were therefore selected for mutation. Lysines (K) 249 and 362 were mutated to alanines (A) using mutagenic primers that flanked the desired lysine and replaced a single nucleotide to change the codon to alanine. A third mutant was designed to contain a double mutation (DM) containing both the 249 and 362 lysine to alanine mutations. Mutants were generated with the QuikChange Lightning PCR Mutagenesis kit (Aligent Technologies) using pcDNA 3.1 DAX-1 wild-type plasmid as template and previously mentioned mutagenesis primers.

Mutant DAX-1 plasmids K249A, K362A, and the double mutant (DM) along with wild-type DAX-1 were expressed with a cell-free expression system and were SUMOylated using an *in vitro* SUMOylation kit. The *in vitro* kit includes reactions for SUMO-1, SUMO-2, and SUMO-3. SUMO-2 and SUMO-3 are difficult to distinguish and are bound by the same antibody. Each reaction includes one isotype of the SUMO protein and the three enzymes required to carry out SUMOylation. The SUMOylated protein samples were then analyzed by western blot (Figure 3-3). Mutation of lysine 249 reduced SUMO-1 binding when compared to WT, K362A, and DM. Interestingly, K362A was reduced for SUMO-2 binding when compared to the WT and other mutants. SUMO-3 had a less clear pattern, however the double mutant appeared to be the most reduced when compared to the WT and single mutants.

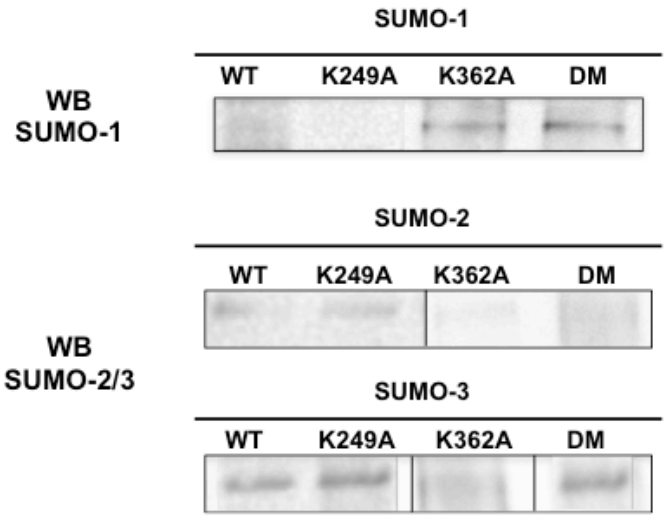

Figure 3-3 *in vitro* SUMOylation of wild-type and SUMO mutant DAX-1.
Four plasmids; wild-type DAX-1 (WT), lysine 249 to alanine mutant DAX-1 (K249), lysine 362 to alanine mutant DAX-1 (K362A), and lysine 249 and 362 to alanine double mutant DAX-1 (DM) were used to produce protein *in vitro*. Protein samples were then SUMOylated using an *in vitro* SUMOylation kit and examined by western blot for the three SUMO types. SUMO-1: K249 had the weakest signal for SUMO-1 indicating that mutation of lysine 249 decreases SUMO-1 binding, and that SUMO-1 may bind preferentially at that site. SUMO-2: K362 had the weakest signal for SUMO-2 indicating that mutation of lysine 362 decreases SUMO-2 binding, and that SUMO-2 may bind preferentially to this site. SUMO-3: K362 had the weakest signal for SUMO-3 indicating that mutation of lysine 362 decreases SUMO-3 binding, and that SUMO-3 may bind preferentially to this site.

Effects of SUMO site mutation of DAX-1 on expression on DAX-1 target genes.

The changes in detectable SUMO level that were observed with the mutants in the *in vitro* SUMOylation experiments indicated that by eliminating K249 and K362, the ability of DAX-1 to become SUMOylated is reduced. This allowed for changes in DAX-1 activity to be examined by comparing mutants to wild-type DAX-1. In order to see how these mutants would change DAX-1's ability to function, DAX-1 mutants were transfected into MCF7 human adenocarcinoma cells. MCF7 cells have low to undetectable endogenous levels of DAX-1. Plasmid transfections of an empty vehicle control (VC), wild-type DAX-1, K249A, K362A, and the double mutant were carried out and these results are shown in Figures 3-4 and 3-5.

Expression levels of GAPDH (control house keeping gene) and DAX-1 were examined by PCR and western blot. Successful transfection of plasmids was confirmed by DAX-1 detection by PCR as shown in Figure 3-4. DAX-1 protein level was also examined (Figure 3-5). Although some DAX-1 protein is detectable in the MCF7 cells, it is far less than what is detected in the WT DAX-1 transfected cells. The level of detectable DAX-1 protein is reduced for the K249A mutant, which may be due to a loss of protein stability resulting from mutation of the SUMOylation site.

Once successful transfection of WT DAX-1 and SUMO mutants of DAX-1 in the MCF7 cells had been confirmed, I sought to examine the effects of SUMOylation of DAX-1 on DAX-1 target gene expression. Of these genes, estrogen receptor alpha and Cyclin D1 were the initial gene targets examined. These targets were chosen because they are regulated by DAX-1, and ectopic expression of DAX-1 in DAX-1 deficient MCF7 breast cancer cells leads to a reduction in ERα and Cyclin D1 transcription (shown in Chapter 2). Expression was assayed by PCR as shown in Figure 3-6. It was observed that cells transfected with WT DAX-1 had reduced

expression levels of both ERα and Cyclin D1 compared to untreated and vehicle control treated cells. As a negative repressor of ERα, this was expected and confirms what was seen previously in the breast cancer proliferation experiments described in Chapter 2.

Interestingly, the single SUMO K249 and K362 mutant transfected cells showed higher expression levels for ERα and Cyclin D1 than the WT DAX-1 transfected cells (Figure 3-6). These results indicate that in cells expressing mutant DAX-1 in which SUMO modifications are inhibited, there was a lack of ERα and Cyclin D1 gene repression. These data suggest that without SUMOylation, DAX-1 is less effective at repressing its target genes. When the double mutant is examined, an even stronger level of repression on ERα and Cyclin D1 is observed. There is less detectable expression of these targets in the cells transfected with the double mutant than what was detected in WT DAX-1 transfected cells (Figure 3-7, Lanes 3 and 6). This is an unexpected result and one that we are seeking to understand in future studies. It was surprising that the two single mutants resulted in a less functional version of DAX-1, but that having both mutations in the same protein led to a version of DAX-1 that appears to be more capable of target gene repression than even the wild-type protein. Perhaps the introduction of two different mutations into the DAX-1 sequence may influence protein folding and could possibly change the overall structure of the protein, causing it to function differently in the MCF7 cells.

Next, I examined downstream proliferation markers Ki-67, MCM7, and TOP2A previously discussed in chapter 2. Ki-67 is a classically used proliferation marker, MCM7 is an S phase protein involved in formation of the replication fork, and TOP2A is an S phase topoisomerase that helps to relieve torsional stress during DNA replication top [70-72]. In cells transfected with wild-type DAX-1, expression of these three proliferation markers was reduced compared to untreated and vehicle control cells

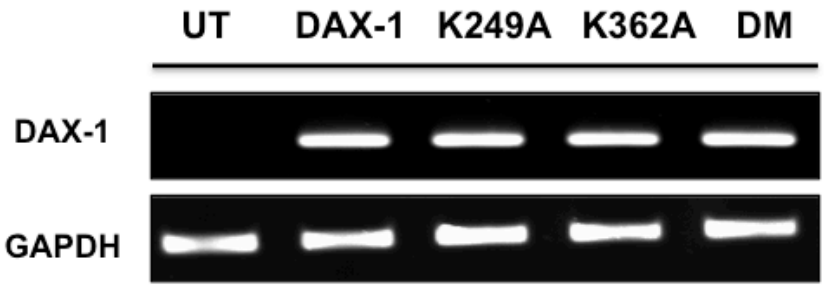

Figure 3-4 cDNA levels of DAX-1 and GAPDH in wild-type and SUMO mutant DAX-1 transfected MCF7 cells.
GAPDH is a PCR control that should not change or be affected by treatment of cells, therefore GAPDH levels should be consistent across all samples and can act as a loading control. PCR of the DAX-1 gene is a way to determine if the transfections were successful. Untreated MCF7 cells typically have very low to undetectable DAX-1 mRNA levels. DAX-1 is only detected in the samples where either wild-type or SUMO mutant DAX-1 was transfected.

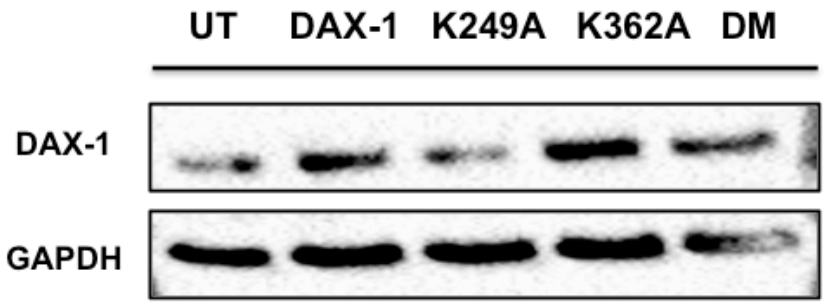

Figure 3-5 Protein levels of DAX-1 and GAPDH in wild-type and SUMO mutant DAX-1 transfected MCF7 cells.
GAPDH is a loading control to determine that the same amount of protein was loaded for each sample. Untreated MCF7 cells have low DAX-1 protein levels. Wild-type DAX-1 transfected cells have higher levels of DAX-1 protein expression. The K249A mutant has less DAX-1 protein than wild-type DAX-1 transfected cells. K362A mutant cells have DAX-1 protein levels similar to wild-type transfected cells and the double mutant has an intermediate amount of DAX-1 protein.

(Figure 3-7, Lanes 1-3). Since DAX-1 is able to repress ERα and reduce the amount of Cyclin D1 being expressed by ERα, reduction of downstream S phase targets genes is expected and was observed previously (see Chapter 2).

When expression of Ki-67, MCM7, and TOP2A was assayed in cells transfected with the SUMO mutation DAX-1, it was found that with the two single mutants, K247 and K362, demonstrated a higher expression level of target genes compared to the WT DAX-1 treated cells (Figure 3-7, Lanes 3-5). A similar result was seen with the ERα and Cyclin D1 genes. Therefore, these results demonstrate that elimination of DAX-1's SUMOylation sites results in a reduction in the ability of DAX-1 to repress target genes. The double mutant DAX-1 transfected cells showed similar expression to the single mutants for Ki-67, and was slightly less for TOP2A (Figure 3-6, Lane 6). However, when expression of MCM7 was examined for the double mutant DAX-1 transfected cells, there was a reduction in expression compared to either the single mutants or the WT DAX-1 transfected cells. This was somewhat unexpected, as it seems unlikely that a double mutant would be more functional than either the single mutants or the wild-type DAX-1. Though this result was similar to what was seen for expression of ERα and Cyclin D1 (Figure 3-7, Lane 6). These results for the SUMO double mutant transfected cells potentially further supports the rationale that there may be some alteration in protein structure that occurs when two different sites are mutated that results in a change in DAX-1 function in MCF7 cells.

Cell cycle analysis of wild-type and SUMO mutant transfected MCF7 breast cancer cells.

Cell cycle analysis by flow cytometry using propidium iodide (PI) staining was used to functionally assess the gene expression data. As described in Chapter 2, cell cycle analysis is a

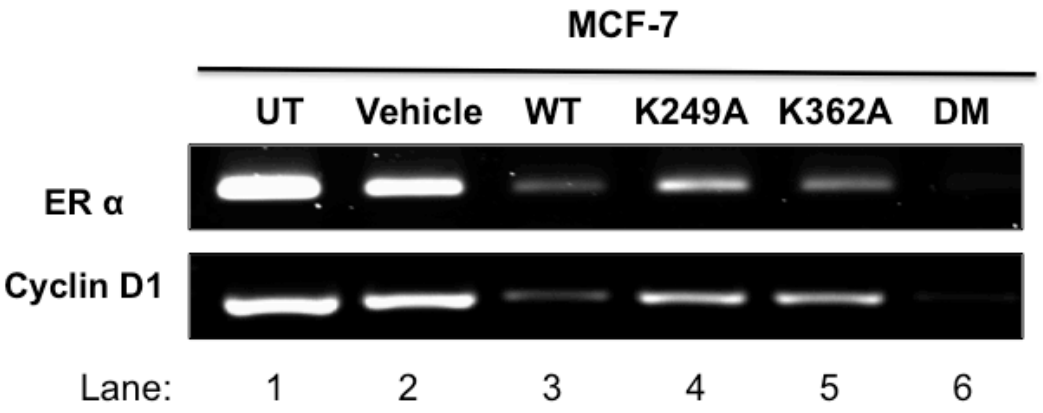

Figure 3-6 cDNA levels of ERα and Cyclin D1 in wild-type and SUMO mutant DAX-1 transfected MCF7 cells.
Expression of wild-type DAX-1 in MCF7 cells leads to a reduction in ERα and Cyclin D1 expression levels. K249A and K362A SUMO mutant transfected cells have lower expression levels of ERα and Cyclin D1 compared to untreated or vehicle control cells (lanes 4 and 5), but higher expression of ERα and Cyclin D1 than wild-type DAX-1 transfected cells. Mutation of the SUMO sites leads to a reduction in DAX-1's ability to repress expression of ERα and Cyclin D1. Expression of the double mutant results in the complete repression of ERα and Cyclin D1 gene expression (lane 6).

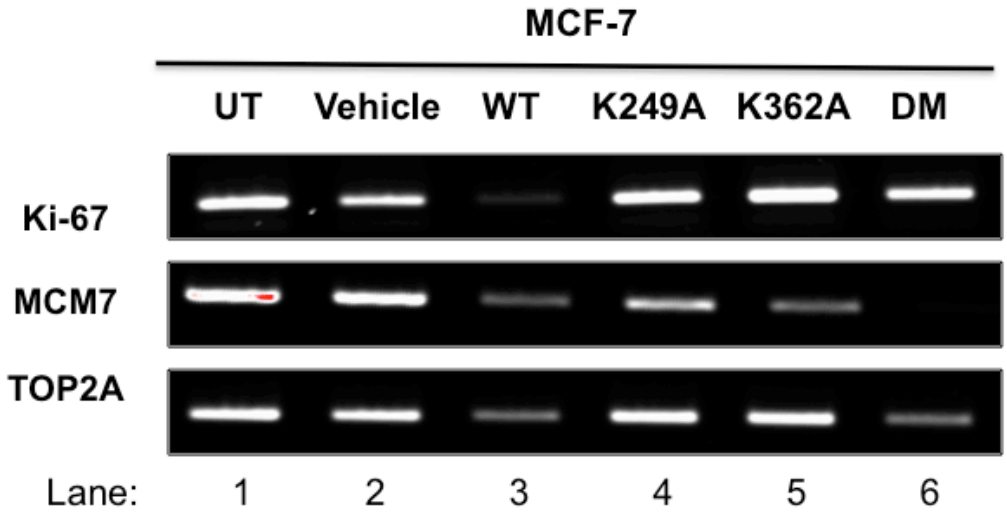

Figure 3-7 cDNA levels of proliferation markers Ki-67, MCM7, and TOP2A in wild-type and SUMO mutant DAX-1 transfected MCF7 cells.
Expression of wild-type DAX-1 in MCF7 cells leads to a reduction in cDNA level for all three proliferation markers Ki-67, MCM7, and TOP2A. K249A and K362A SUMO mutant transfected cells have similar Ki-67 and TOP2A expression levels as cells that are untreated and vehicle control cells. Expression levels of MCM7 in cells transfected with K249A and K362A mutant DAX-1 were lower than untreated and vehicle control cells. Therefore, mutating SUMO sites leads to some reduction in DAX-1's ability to repress expression of Ki-67, MCM7, and TOP2A. The double mutant does not exhibit a clear pattern for these three proliferation genes. The double mutant is comparable with the K249A and K362A for Ki-67, but completely represses expression of MCM7 and has a similar cDNA level with wild-type DAX-1 for TOP2A.

method of distinguishing what stage of the cell cycle different populations of cells are in at the time of analysis. MCF7 cells were left untreated or transfected with either vehicle control, wild-type DAX-1, K249A mutant, K362A mutant, or double mutant plasmids. Following a 48 hour incubation, cells were collected, stained with PI, and analyzed via flow cytometry. As had been previously observed in the experiments in Chapter 2, there was a shift in the wild-type DAX-1 treated cells, which was found to be statistically significant ($p = .018$). Specifically, more cells were found to be in G0/G1 compared to untreated or vehicle control cells (Figure 3-8a). There were 24.2% and 24.7% of cells in G0/G1 for untreated and vehicle control groups respectively and 28.9% of cells in G0/G1 for WT DAX-1 treated cells (Figure 3-8b). These data supports my previous expression data demonstrating that ERα and Cyclin D1 repression by DAX-1 causes more cells to stay in G0/G1 rather than progressing to S phase. Compared to WT DAX-1, no significant shift was seen with the SUMO mutants (Figure 3-8a). Cells transfected with the K249A, K362A, and double mutant behaved much like the untreated and vehicle control cells. When compared with WT DAX-1 cells, a significant shift in percentage of cells in G1/G0 was observed in the K249A ($p = .026$), K362A ($p = .047$), and double mutants ($p = .047$). Percentages of cells in G0/G1 were 22.9%, 24.4% and 25.4% for the K249A, K362A, and double mutant respectively (Figure 3-8b). Interestingly, loss of SUMO binding sites appears to change the function or stability of DAX-1, at least to some degree. The repression in proliferation observed with wild-type DAX-1 is lost when SUMO sites are mutated, supporting previous expression data, with the K249A and K362A mutants. Inhibition of proliferative genes observed with wild-type DAX-1 transfected cells was reduced when cells were transfected with K249A and K362A SUMO mutant DAX-1. Similarly, the inhibition of proliferation seen with wild-type DAX-1

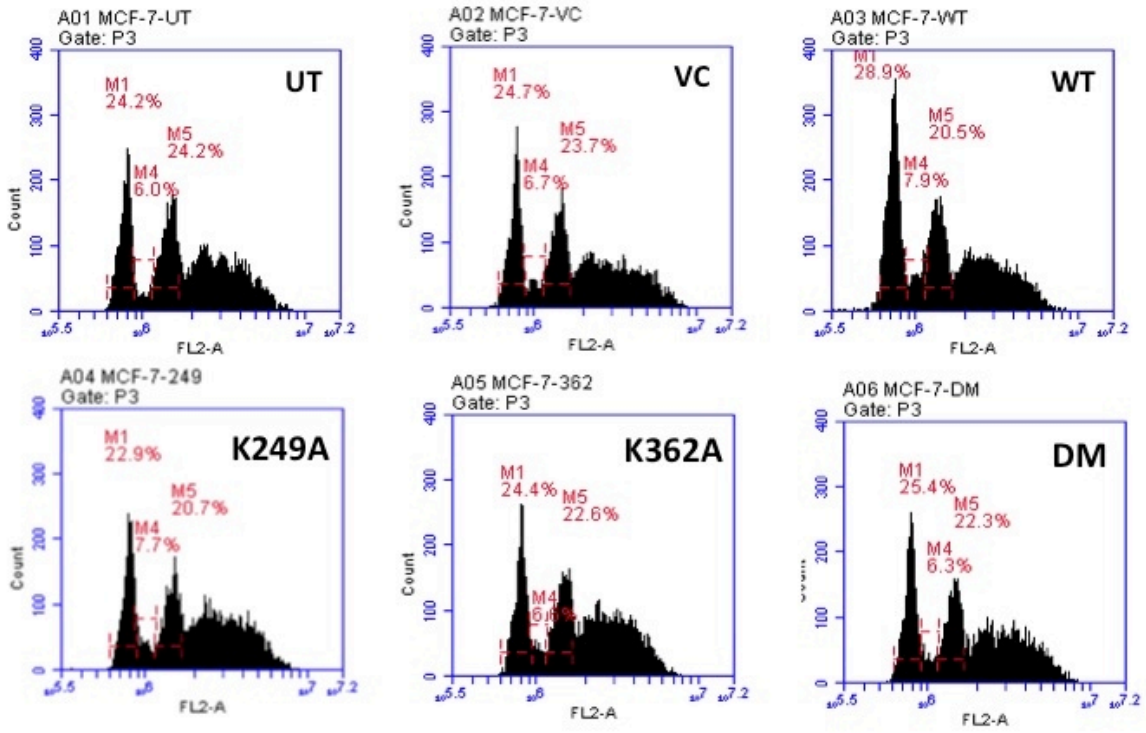

Figure 3-8a Cell cycle analysis of wild-type and SUMO mutant DAX-1 transfected MCF7 cells.

Wild-type DAX-1 transfected cells had an increase in the proportion of cells in G0/G1 of the cells cycle when compared with untreated or vehicle control cells. The proportion of cells in G0/G1 for DAX-1 SUMO mutant transfected cells was more similar to untreated and vehicle control cells. UT: untreated VC: vehicle control WT: wild-type DAX-1 K249A: K249A SUMO mutant K362A: K362A SUMO mutant DM: double mutant. First peak in histogram represents proportion of cells in G0/G1 phase of cell cycle and the second peak represents cells in G2/M phase of cell cycle.

(Refer to Chapter 2 for diagram of cell cycle analysis methodology)

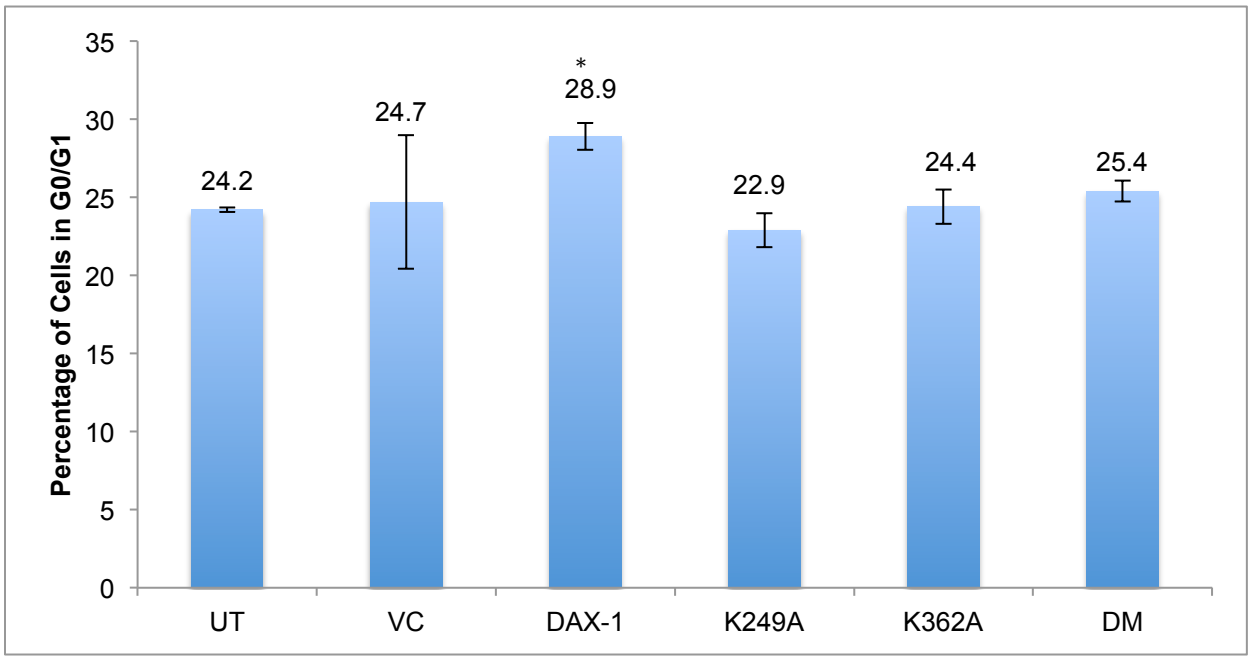

Figure 3-8b Quantification of cell cycle analysis of wild-type and SUMO mutant DAX-1 transfected cells.
Quantification of cell cycle analysis data shown in Figure 3-8a, graph represents proportion of cells for each treatment group that were in G0/G1 of the cell cycle.
P<0.05 *

transfected cells was lost when cells were transfected with K249A and K362A SUMO mutant DAX-1.

Apoptosis analysis by annexin V of wild-type and SUMO mutant DAX-1 transfected MCF7 breast cancer cells.

I have shown that DAX-1 acts to slow growth and proliferation through repression of ERα and its transcription target Cyclin D1. However, it is unknown if DAX-1 plays any role in apoptosis. The goal of these experiments was to determine if expression of DAX-1 induces apoptosis more readily than untreated cells and to evaluate differences between the action of wild-type DAX-1 compared to the DAX-1 SUMO mutants.

Apoptosis analysis involves fluorescence detection of Annexin V and PI to determine whether cells are healthy or if they are entering early or late stage apoptosis [73, 74]. Annexin V stains phosphatidylserine (PS), a phospholipid membrane component that is only found on the inner leaflet of the cell membrane in healthy cells. During early apoptosis, phosphatidylserine flips from the inner layer of the membrane to the outer layer of the membrane. Cells that are positive for Annexin V staining are in the early stages of apoptosis. Propidium iodide (PI) stains DNA and can only penetrate cells that have lost membrane integrity due to late stage apoptosis or necrosis. Cells that stain for Annexin V alone are in early apoptosis. Cells with both Annexin and PI staining are in the later stages of apoptosis. Cells stained with PI alone have undergone some mechanical damage or are necrotic. A sample plot is shown in Figure 3-9.

In these experiments the focus was primarily on cells entering early and late stages of apoptosis. MCF7 cells were transfected as before, with either vehicle control, wild-type DAX-1, or SUMO mutant DAX-1 (in pcDNA3.1) and incubated for 48 hours before collection. Collected cells were co-stained with Annexin V and PI prior to stain detection by flow cytometry.

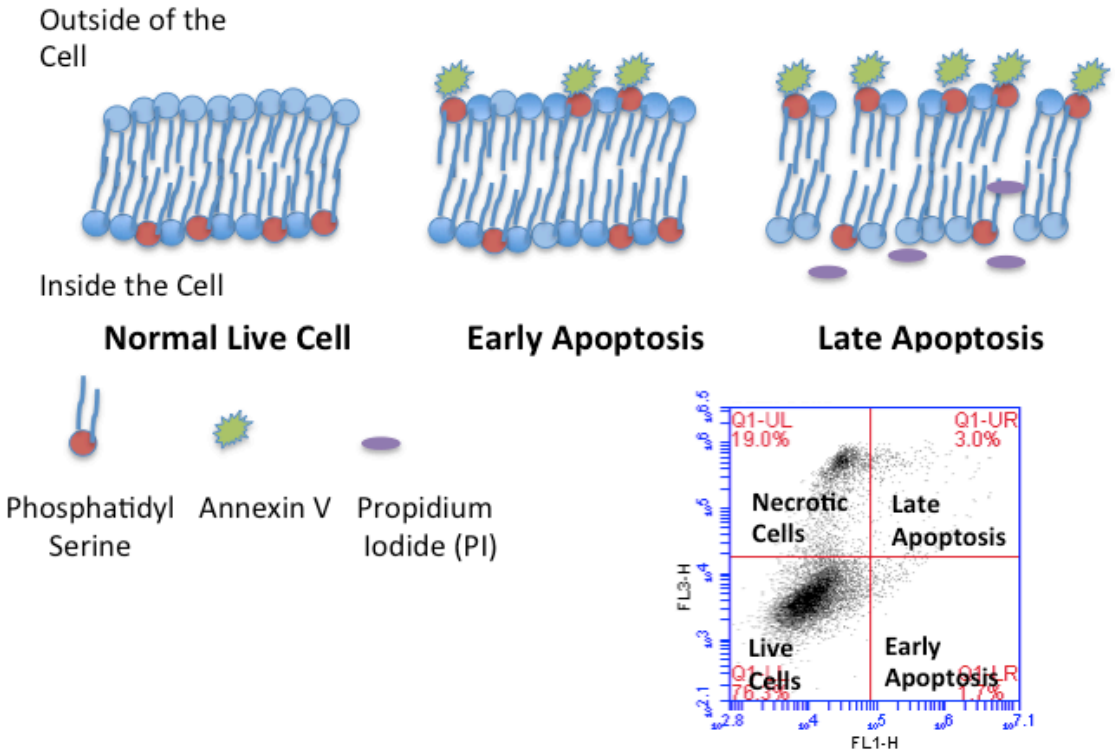

Figure 3-9 Annexin V/PI apoptosis analysis diagram.
Normally phosphatidylserine is found only on the inner leaflet of the plasma membrane, however during early stages of apoptosis phosphatidylserine flips from the inner to the outer leaflet of the membrane. Annexin V stains phosphatidylserine and produces a signal detectable by flow cytometry. PI stains DNA and cannot enter cells unless a loss of membrane integrity has occurred. Loss of membrane integrity can be attributed to late stage apoptosis or necrosis. Viable cells without any staining will localize to the lower left quadrant. Cell with only PI staining are necrotic and will be found in the upper left quadrant. Cell in early apoptosis will stain with for Annexin V only and will be found in the lower right quadrant. Cells in later stages of apoptosis will have co-staining for both Annexin V and PI and will be found in the upper right quadrant.

Untreated and vehicle control cells yielded similar plots with 1.8% (UT) and 1.7% (VC) of cells in early apoptosis and 4.4% (UT) and 3.0% (VC) in late apoptosis (Figure 3-10a and b). Wild-type DAX-1 expressing cells presented a strong shift with 33.0% of cells in early apoptosis and 8.1% of cells in late apoptosis (Figure 3-10a and b). The SUMO mutant transfected cells more closely resembled the UT and VC cells compared to the WT DAX-1 treated cells. SUMO mutant DAX-1 treated cells had 5.5% (K249A), 5.7% (K362A), and 0.6% (DM) of cells in early apoptosis and 5.6% (K249A), 7.4% (K362A), and 2.3% (DM) of cells in later apoptosis (Figure 3-10a and b). The single mutants had greater populations of cells in early and late apoptosis than untreated and vehicle control cells, but had far fewer cells in early apoptosis than wild-type DAX-1 cells. The double mutant had values that were a closer match to the untreated and control cells for early and late apoptosis.

These data echo what was seen in previous experiments performed with the DAX-1 SUMO mutants. With SUMO sites mutated, DAX-1 is unable to function as it does in its native state. The repressive ability of DAX-1 is reduced with the mutations, as is the ability of DAX-1 to slow proliferation and induce apoptosis. While still preliminary, the apoptosis data indicates that DAX-1 may have a role not only in proliferation, but also in programed cell death. More studies into the role of DAX-1 are needed and are part of future experiments to be carried out in the Tzagarakis-Foster lab.

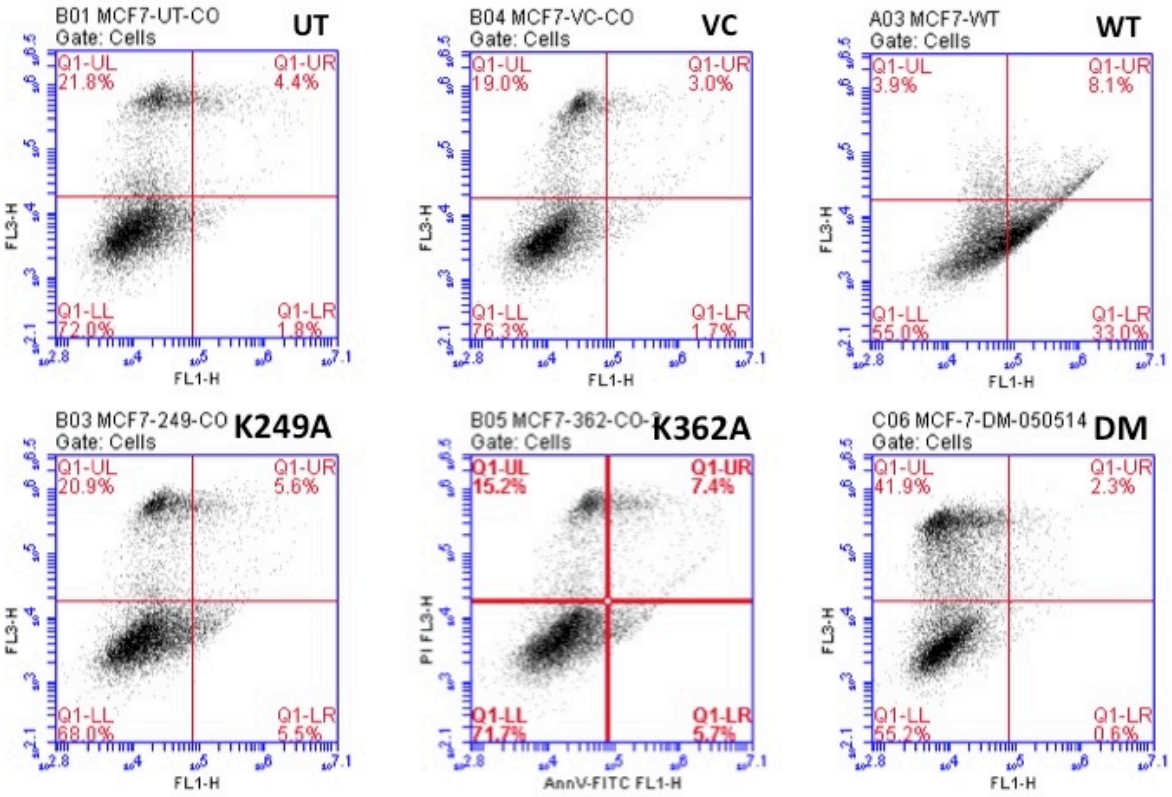

Figure 3-10a Apoptosis analysis of wild-type and SUMO mutant DAX-1 transfected cells by Annexin V/PI staining.
Wild-type DAX-1 transfected cells produced a strong shift in proportion of cells undergoing early apoptosis. SUMO mutants K249A and K362A had a small shift, but overall had a distribution that was more similar to untreated and vehicle control cells than to wild-type DAX-1 transfected cells. The double mutant transfected cells had similar distributions of cells in early and late apoptosis, but had more cells than any other treatment group undergoing necrosis. UT: untreated VC: vehicle control WT: wild-type DAX-1 K249A: K249A SUMO mutant K362A: K362A SUMO mutant DM: double mutant.

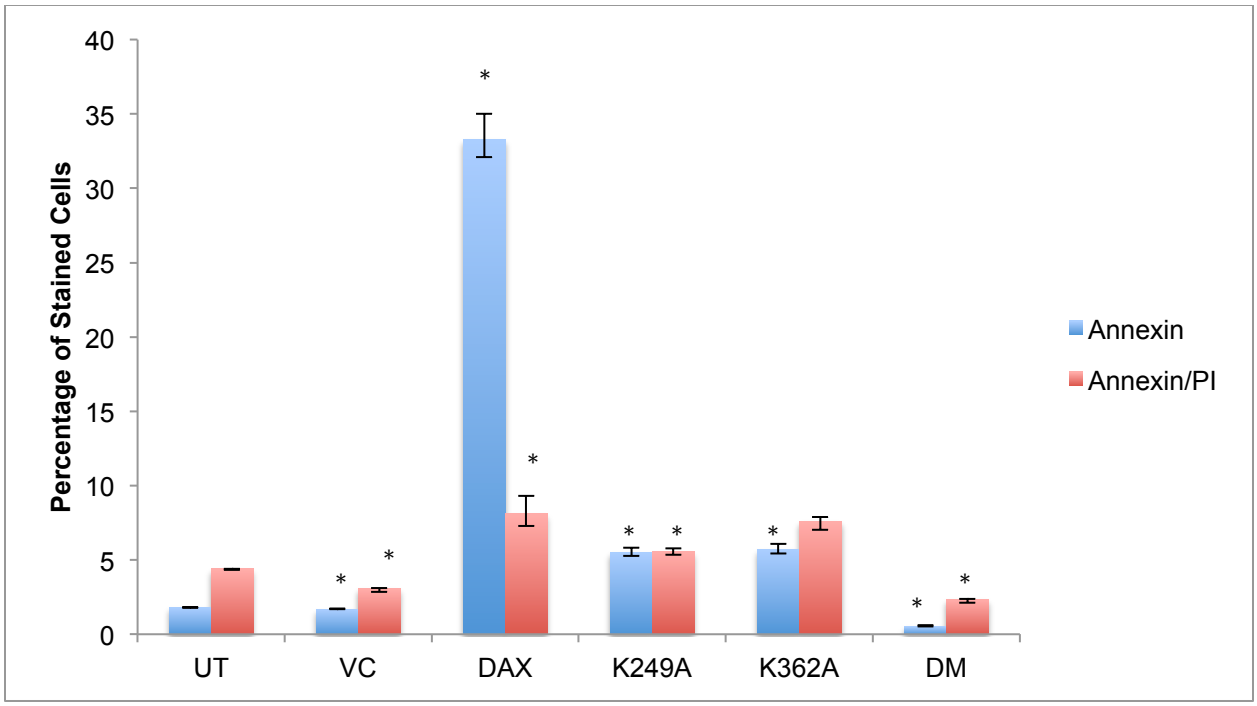

Figure 3-10b Quantification of Apoptosis analysis in wild-type and DAX-1 SUMO mutant transfected cells by Annexin V/PI staining.
Quantification of proportion of cells in each treatment group stained with Annexin V (early apoptosis) or Annexin V and PI (late apoptosis). Annexin V: UT 1.8%, VC 1.7%, DAX 33%, K249A 5.5%, K362A 5.7%, and DM 0.6%. Annexin/PI: UT 4.4%, VC 3.0%, DAX 8.1%, K249A 5.6%, K362A7.4%, and DM 2.3%. Significance based on comparison of UT and transfected groups for staining of Annexin V alone or Annexin V and PI.
$P<0.05$ *

Chapter 3: Discussion and Future Directions

SUMOylation of target proteins has been shown to have a variety of effects and may play a critical role in regulating function. Research has shown that mutation of the SUMO sites within SF-1, an NHR closely related to DAX-1, resulted in abnormal endocrine development [69, 75, 76]. These studies influenced our desire to determine the SUMOylation status of DAX-1 and to elucidate the effect that SUMOylation has on the function of DAX-1. In this research, I determined that DAX-1 is, in fact, SUMOylated in cell lines and that mutation of predicted SUMO sites resulted in changes in DAX-1's ability to repress transcription of target genes. Wild-type DAX-1 is able to repress the transcriptional activity of ERα, thereby reducing the expression of Cyclin D1, a direct target of ERα. When the predicted SUMO sites within DAX-1, K249 and K361, were mutated, repression of ERα and Cyclin D1 was reduced when compared with WT DAX-1. This helps to support the hypothesis that SUMOylation of DAX-1 is important for its proper function. A similar result was seen when three S phase proliferation markers were examined. That is, expression of WT DAX-1 reduced the expression of these genes, whereas the expression of the single DAX-1 SUMO mutants led to a reduction in repression compared to WT DAX-1.

There were unexpected results obtained with the DAX-1 SUMO double mutant. Specifically, ERα, Cyclin D1, MCM7, and TOP2A were repressed to a greater degree when the double mutant was expressed than they were with WT DAX-1. Interestingly, for Ki-67, the double mutant had a similar level of expression to the single mutants K249A and K362A. The variation seen with the double mutant was unexpected, as was the fact that for the majority of the targets tested the double mutant reduced expression of the proliferation markers more than WT

DAX-1. One possible explanation for this observation is that by changing two lysine residues to alanines, we have unintentionally changed the folding and three-dimensional shape of DAX-1. Lysine is a positively charged amino acid, whereas alanine is a non-polar amino acid. Therefore, changing lysine residues to alanine could potentially change the way a particular region of the DAX-1 protein folds. Perhaps changing these to two residues shifted the positioning of the protein such that it is able to bind more tightly to the promoter region of ERα and prevent transcription. In order to address the issues that arose with the double K to A mutant more experiments will be conducted.

For example, since there are unintended consequences of replacing positively charged lysine with non-polar alanine, additional mutants are being constructed that replace lysine with arginine (R). Arginine is positively charged and is much more similar to lysine than alanine. Future SUMOylation studies will be performed using K249R, K362R, and R double mutants. These studies will help to confirm that mutation of putative SUMO sites change the function of DAX-1 and leads to a reduction in repressional ability. Additionally, these experiments should help to explain the results that were observed using the alanine double SUMO mutant, specifically to address if the inconsistencies were due to some conformational changes from alanine or if there is some unknown consequence of mutating both putative SUMO sites.

The apoptosis analysis data for wild-type DAX-1 was quite striking and needs to be further explored. Other research in the Tzagarakis-Foster laboratory has revealed interactions with DAX-1 and the apoptotic Bcl-2 family. To date, research with DAX-1 has been primarily focused on proliferation, however this preliminary data suggests that DAX-1 may play an even more significant role in promoting apoptosis by way of repressing anti-apoptotic genes. This may be a very promising new avenue to explore in DAX-1 research.

References

1. Sablin, E.P., et al., *The structure of corepressor Dax-1 bound to its target nuclear receptor LRH-1.* Proc Natl Acad Sci U S A, 2008. **105**(47): p. 18390-5.
2. McEwan, I.J. and A.M. Nardulli, *Nuclear hormone receptor architecture - form and dynamics: The 2009 FASEB Summer Conference on Dynamic Structure of the Nuclear Hormone Receptors.* Nucl Recept Signal, 2009. **7**: p. e011.
3. Watson, P.J., L. Fairall, and J.W. Schwabe, *Nuclear hormone receptor co-repressors: structure and function.* Mol Cell Endocrinol, 2012. **348**(2): p. 440-9.
4. Steinmetz, A.C., J.P. Renaud, and D. Moras, *Binding of ligands and activation of transcription by nuclear receptors.* Annu Rev Biophys Biomol Struct, 2001. **30**: p. 329-59.
5. Warnmark, A., et al., *Activation functions 1 and 2 of nuclear receptors: molecular strategies for transcriptional activation.* Mol Endocrinol, 2003. **17**(10): p. 1901-9.
6. Bishop, T.C., D. Kosztin, and K. Schulten, *How hormone receptor-DNA binding affects nucleosomal DNA: the role of symmetry.* Biophys J, 1997. **72**(5): p. 2056-67.
7. Kosztin, D., T.C. Bishop, and K. Schulten, *Binding of the estrogen receptor to DNA. The role of waters.* Biophys J, 1997. **73**(2): p. 557-70.
8. Mangelsdorf, D.J., et al., *The nuclear receptor superfamily: the second decade.* Cell, 1995. **83**(6): p. 835-9.
9. Guo, W., T.P. Burris, and E.R. McCabe, *Expression of DAX-1, the gene responsible for X-linked adrenal hypoplasia congenita and hypogonadotropic hypogonadism, in the hypothalamic-pituitary-adrenal/gonadal axis.* Biochem Mol Med, 1995. **56**(1): p. 8-13.
10. Burris, T.P., W. Guo, and E.R. McCabe, *The gene responsible for adrenal hypoplasia congenita, DAX-1, encodes a nuclear hormone receptor that defines a new class within the superfamily.* Recent Prog Horm Res, 1996. **51**: p. 241-59; discussion 259-60.
11. Niakan, K.K., et al., *Novel role for the orphan nuclear receptor Dax1 in embryogenesis, different from steroidogenesis.* Mol Genet Metab, 2006. **88**(3): p. 261-71.
12. Niakan, K.K. and E.R. McCabe, *DAX1 origin, function, and novel role.* Mol Genet Metab, 2005. **86**(1-2): p. 70-83.
13. Zanaria, E., et al., *An unusual member of the nuclear hormone receptor superfamily responsible for X-linked adrenal hypoplasia congenita.* Nature, 1994. **372**(6507): p. 635-41.
14. Suzuki, T., et al., *LXXLL-related motifs in Dax-1 have target specificity for the orphan nuclear receptors Ad4BP/SF-1 and LRH-1.* Mol Cell Biol, 2003. **23**(1): p. 238-49.
15. Hanley, N.A., et al., *Expression profiles of SF-1, DAX1, and CYP17 in the human fetal adrenal gland: potential interactions in gene regulation.* Mol Endocrinol, 2001. **15**(1): p. 57-68.
16. Iyer, A.K., Y.H. Zhang, and E.R. McCabe, *LXXLL motifs and AF-2 domain mediate SHP (NR0B2) homodimerization and DAX1 (NR0B1)-DAX1A heterodimerization.* Mol Genet Metab, 2007. **92**(1-2): p. 151-9.

17. Zhang, H., et al., *DAX-1 functions as an LXXLL-containing corepressor for activated estrogen receptors.* J Biol Chem, 2000. **275**(51): p. 39855-9.
18. Ito, M., R. Yu, and J.L. Jameson, *DAX-1 inhibits SF-1-mediated transactivation via a carboxy-terminal domain that is deleted in adrenal hypoplasia congenita.* Mol Cell Biol, 1997. **17**(3): p. 1476-83.
19. Ikeda, Y., et al., *Steroidogenic factor 1 and Dax-1 colocalize in multiple cell lineages: potential links in endocrine development.* Mol Endocrinol, 1996. **10**(10): p. 1261-72.
20. Nachtigal, M.W., et al., *Wilms' tumor 1 and Dax-1 modulate the orphan nuclear receptor SF-1 in sex-specific gene expression.* Cell, 1998. **93**(3): p. 445-54.
21. Song, K.H., et al., *The atypical orphan nuclear receptor DAX-1 interacts with orphan nuclear receptor Nur77 and represses its transactivation.* Mol Endocrinol, 2004. **18**(8): p. 1929-40.
22. Agoulnik, I.U., et al., *Repressors of androgen and progesterone receptor action.* J Biol Chem, 2003. **278**(33): p. 31136-48.
23. Crawford, P.A., et al., *Nuclear receptor DAX-1 recruits nuclear receptor corepressor N-CoR to steroidogenic factor 1.* Mol Cell Biol, 1998. **18**(5): p. 2949-56.
24. Nakae, J., et al., *Three novel mutations and a de novo deletion mutation of the DAX-1 gene in patients with X-linked adrenal hypoplasia congenita.* J Clin Endocrinol Metab, 1997. **82**(11): p. 3835-41.
25. Iyer, A.K. and E.R. McCabe, *Molecular mechanisms of DAX1 action.* Mol Genet Metab, 2004. **83**(1-2): p. 60-73.
26. Phelan, J.K. and E.R. McCabe, *Mutations in NR0B1 (DAX1) and NR5A1 (SF1) responsible for adrenal hypoplasia congenita.* Hum Mutat, 2001. **18**(6): p. 472-87.
27. Zhang, Y.H., et al., *Nine novel mutations in NR0B1 (DAX1) causing adrenal hypoplasia congenita.* Hum Mutat, 2001. **18**(6): p. 547.
28. Iyer, A.K., Y.H. Zhang, and E.R. McCabe, *Dosage-sensitive sex reversal adrenal hypoplasia congenita critical region on the X chromosome, gene 1 (DAX1) (NR0B1) and small heterodimer partner (SHP) (NR0B2) form homodimers individually, as well as DAX1-SHP heterodimers.* Mol Endocrinol, 2006. **20**(10): p. 2326-42.
29. Jo, Y. and D.M. Stocco, *Regulation of steroidogenesis and steroidogenic acute regulatory protein in R2C cells by DAX-1 (dosage-sensitive sex reversal, adrenal hypoplasia congenita, critical region on the X chromosome, gene-1).* Endocrinology, 2004. **145**(12): p. 5629-37.
30. Stocco, D.M. and B.J. Clark, *Role of the steroidogenic acute regulatory protein (StAR) in steroidogenesis.* Biochem Pharmacol, 1996. **51**(3): p. 197-205.
31. Stocco, D.M. and B.J. Clark, *The role of the steroidogenic acute regulatory protein in steroidogenesis.* Steroids, 1997. **62**(1): p. 29-36.
32. Liu, J., et al., *Expression of the steroidogenic acute regulatory protein mRNA in adrenal tumors and cultured adrenal cells.* J Endocrinol, 1996. **150**(1): p. 43-50.
33. Zazopoulos, E., et al., *DNA binding and transcriptional repression by DAX-1 blocks steroidogenesis.* Nature, 1997. **390**(6657): p. 311-5.
34. Conde, I., et al., *DAX-1 expression in human breast cancer: comparison with estrogen receptors ER-alpha, ER-beta and androgen receptor status.* Breast Cancer Res, 2004. **6**(3): p. R140-8.

35. Wong, C.W., B. Komm, and B.J. Cheskis, *Structure-function evaluation of ER alpha and beta interplay with SRC family coactivators. ER selective ligands.* Biochemistry, 2001. **40**(23): p. 6756-65.
36. Cheng, G., et al., *Estrogen receptors ER alpha and ER beta in proliferation in the rodent mammary gland.* Proc Natl Acad Sci U S A, 2004. **101**(11): p. 3739-46.
37. Arnold, A. and A. Papanikolaou, *Cyclin D1 in breast cancer pathogenesis.* J Clin Oncol, 2005. **23**(18): p. 4215-24.
38. Lanzino, M., et al., *Inhibition of cyclin D1 expression by androgen receptor in breast cancer cells--identification of a novel androgen response element.* Nucleic Acids Res, 2010. **38**(16): p. 5351-65.
39. Hui, R., et al., *Constitutive overexpression of cyclin D1 but not cyclin E confers acute resistance to antiestrogens in T-47D breast cancer cells.* Cancer Res, 2002. **62**(23): p. 6916-23.
40. Lanzino, M., et al., *DAX-1, as an androgen-target gene, inhibits aromatase expression: a novel mechanism blocking estrogen-dependent breast cancer cell proliferation.* Cell Death Dis, 2013. **4**: p. e724.
41. Birrell, S.N., R.E. Hall, and W.D. Tilley, *Role of the androgen receptor in human breast cancer.* J Mammary Gland Biol Neoplasia, 1998. **3**(1): p. 95-103.
42. Somboonporn, W. and S.R. Davis, *Postmenopausal testosterone therapy and breast cancer risk.* Maturitas, 2004. **49**(4): p. 267-75.
43. Missmer, S.A., et al., *Endogenous estrogen, androgen, and progesterone concentrations and breast cancer risk among postmenopausal women.* J Natl Cancer Inst, 2004. **96**(24): p. 1856-65.
44. Zhang, H., et al., *The prognostic value of the orphan nuclear receptor DAX-1 (NROB1) in node-negative breast cancer.* Anticancer Res, 2011. **31**(2): p. 443-9.
45. Holter, E., et al., *Inhibition of androgen receptor (AR) function by the reproductive orphan nuclear receptor DAX-1.* Mol Endocrinol, 2002. **16**(3): p. 515-28.
46. Meluh, P.B. and D. Koshland, *Evidence that the MIF2 gene of Saccharomyces cerevisiae encodes a centromere protein with homology to the mammalian centromere protein CENP-C.* Mol Biol Cell, 1995. **6**(7): p. 793-807.
47. Shen, Z., et al., *UBL1, a human ubiquitin-like protein associating with human RAD51/RAD52 proteins.* Genomics, 1996. **36**(2): p. 271-9.
48. Okura, T., et al., *Protection against Fas/APO-1- and tumor necrosis factor-mediated cell death by a novel protein, sentrin.* J Immunol, 1996. **157**(10): p. 4277-81.
49. Matunis, M.J., E. Coutavas, and G. Blobel, *A novel ubiquitin-like modification modulates the partitioning of the Ran-GTPase-activating protein RanGAP1 between the cytosol and the nuclear pore complex.* J Cell Biol, 1996. **135**(6 Pt 1): p. 1457-70.
50. Mahajan, R., et al., *A small ubiquitin-related polypeptide involved in targeting RanGAP1 to nuclear pore complex protein RanBP2.* Cell, 1997. **88**(1): p. 97-107.
51. Geiss-Friedlander, R. and F. Melchior, *Concepts in sumoylation: a decade on.* Nat Rev Mol Cell Biol, 2007. **8**(12): p. 947-56.
52. Melchior, F., *SUMO--nonclassical ubiquitin.* Annu Rev Cell Dev Biol, 2000. **16**: p. 591-626.
53. Guo, D., et al., *A functional variant of SUMO4, a new I kappa B alpha modifier, is associated with type 1 diabetes.* Nat Genet, 2004. **36**(8): p. 837-41.

54. Rosas-Acosta, G., et al., *A universal strategy for proteomic studies of SUMO and other ubiquitin-like modifiers.* Mol Cell Proteomics, 2005. **4**(1): p. 56-72.
55. Vertegaal, A.C., et al., *Distinct and overlapping sets of SUMO-1 and SUMO-2 target proteins revealed by quantitative proteomics.* Mol Cell Proteomics, 2006. **5**(12): p. 2298-310.
56. Schimmel, J., et al., *The ubiquitin-proteasome system is a key component of the SUMO-2/3 cycle.* Mol Cell Proteomics, 2008. **7**(11): p. 2107-22.
57. Baek, S.H., *A novel link between SUMO modification and cancer metastasis.* Cell Cycle, 2006. **5**(14): p. 1492-5.
58. Desterro, J.M., et al., *Identification of the enzyme required for activation of the small ubiquitin-like protein SUMO-1.* J Biol Chem, 1999. **274**(15): p. 10618-24.
59. Okuma, T., et al., *In vitro SUMO-1 modification requires two enzymatic steps, E1 and E2.* Biochem Biophys Res Commun, 1999. **254**(3): p. 693-8.
60. Gong, L., et al., *Molecular cloning and characterization of human AOS1 and UBA2, components of the sentrin-activating enzyme complex.* FEBS Lett, 1999. **448**(1): p. 185-9.
61. Tatham, M.H., et al., *Polymeric chains of SUMO-2 and SUMO-3 are conjugated to protein substrates by SAE1/SAE2 and Ubc9.* J Biol Chem, 2001. **276**(38): p. 35368-74.
62. Sharrocks, A.D., *PIAS proteins and transcriptional regulation--more than just SUMO E3 ligases?* Genes Dev, 2006. **20**(7): p. 754-8.
63. Takahashi, Y., et al., *Yeast Ull1/Siz1 is a novel SUMO1/Smt3 ligase for septin components and functions as an adaptor between conjugating enzyme and substrates.* J Biol Chem, 2001. **276**(52): p. 48973-7.
64. Zhao, X. and G. Blobel, *A SUMO ligase is part of a nuclear multiprotein complex that affects DNA repair and chromosomal organization.* Proc Natl Acad Sci U S A, 2005. **102**(13): p. 4777-82.
65. Zunino, R., et al., *The SUMO protease SENP5 is required to maintain mitochondrial morphology and function.* J Cell Sci, 2007. **120**(Pt 7): p. 1178-88.
66. Kim, K.I., S.H. Baek, and C.H. Chung, *Versatile protein tag, SUMO: its enzymology and biological function.* J Cell Physiol, 2002. **191**(3): p. 257-68.
67. Ying, S., et al., *Estrogen receptor alpha and nuclear factor Y coordinately regulate the transcription of the SUMO-conjugating UBC9 gene in MCF-7 breast cancer cells.* PLoS One, 2013. **8**(9): p. e75695.
68. Yu, E.J., et al., *SUMOylation of ZFP282 potentiates its positive effect on estrogen signaling in breast tumorigenesis.* Oncogene, 2013. **32**(35): p. 4160-8.
69. Lee, F.Y., et al., *Eliminating SF-1 (NR5A1) sumoylation in vivo results in ectopic hedgehog signaling and disruption of endocrine development.* Dev Cell, 2011. **21**(2): p. 315-27.
70. Tubbs, R., et al., *Outcome of patients with early-stage breast cancer treated with doxorubicin-based adjuvant chemotherapy as a function of HER2 and TOP2A status.* J Clin Oncol, 2009. **27**(24): p. 3881-6.
71. Endl, E. and J. Gerdes, *The Ki-67 protein: fascinating forms and an unknown function.* Exp Cell Res, 2000. **257**(2): p. 231-7.
72. Wei, Q., et al., *Phosphorylation of minichromosome maintenance protein 7 (MCM7) by cyclin/cyclin-dependent kinase affects its function in cell cycle regulation.* J Biol Chem, 2013. **288**(27): p. 19715-25.

73. van Engeland, M., et al., *A novel assay to measure loss of plasma membrane asymmetry during apoptosis of adherent cells in culture.* Cytometry, 1996. **24**(2): p. 131-9.
74. Casciola-Rosen, L., et al., *Surface blebs on apoptotic cells are sites of enhanced procoagulant activity: implications for coagulation events and antigenic spread in systemic lupus erythematosus.* Proc Natl Acad Sci U S A, 1996. **93**(4): p. 1624-9.
75. Lee, M.B., et al., *The DEAD-box protein DP103 (Ddx20 or Gemin-3) represses orphan nuclear receptor activity via SUMO modification.* Mol Cell Biol, 2005. **25**(5): p. 1879-90.
76. Campbell, L.A., et al., *Decreased recognition of SUMO-sensitive target genes following modification of SF-1 (NR5A1).* Mol Cell Biol, 2008. **28**(24): p. 7476-86.